ORIGINAL PAPER

A Simplistic Method for Assessing Seismic Damage in Rock Tunnels Before Earthquake: Part 1—Damage Prediction and Validation Using Seismic Damage Classification of Tunnels

A. Dinesh Reddy[1] · Aditya Singh[1]

Abstract

Numerous researchers worked on classifying the post-earthquake damages in tunnels. These post-earthquake damage classifications are modified by researchers for every seismic event based on the amount of damage. To establish a uniform damage classification, a large amount of data is necessary from various seismic events. To date, there are no specific guidelines to assess the seismic damage of tunnels. In this study, a simplistic method is proposed to predict and assess the seismic damage to the rock tunnels before an earthquake using the seismic damage classification of tunnels (SDCT). To overcome the limitations of previous studies, the largest global seismic damage database of tunnels (SDDT) is created, using actual damage data from 235 damaged tunnel sites from 26 different earthquakes. This study introduces three things. First, a simple SDCT is proposed using the SDDT. In the SDCT, seismic damages to a tunnel are categorized as damages incurred in a tunnel at three locations namely lining, portal, and invert. Based on SDCT, seven damage classes ranging from extremely high (EH) to extremely low (EL) are proposed. Every class has damage categories with detailed damage descriptions and are also linked to the influence parameters (seismic, geological, and structural) of a tunnel. Second, a critical combination of the seven influence parameters is identified in each damage class for predicting the damage category of lining, portal, and invert of SDCT. Therefore, for the first time before an earthquake, the proposed SDCT can predict and assess the seismic damages to the rock tunnels. Third, a simple methodology is proposed based on the critical combination of seven influence parameters. This simplistic method can identify the seismic vulnerability of rock tunnels (SVRT) before an earthquake. The proposed simplistic methodology clearly distinguishes the levels of seismic, geological, and structural parameters in each damage class. This helps engineers predict the damage type and amount of damage corresponding to the damage class before an earthquake at the site. This methodology helps the engineers to develop the seismic parameters initially and understand the seismic environment of the site. After developing the seismic parameters and utilizing the geological, and structural parameters at the site, engineers can clearly outline the predicted damages. The proposed methodology does not require complex mathematical calculations and modeling, it can be used by the engineers for preliminary investigations. The validation of the proposed methodology was done to the Erkenek tunnel situated in Türkiye, which showed a good agreement with the proposed methodology.

✉ Aditya Singh
aditya.singh@ce.iitr.ac.in

A. Dinesh Reddy
dinesh_r@ce.iitr.ac.in

1   Department of Civil Engineering, Indian Institute
    of Technology Roorkee, Roorkee, Uttarakhand 247667, India

Highlights

- For the first time, a simple method is proposed for predicting and assessing the seismic damages to the rock tunnels before an earthquake using the seismic damage classification of tunnels (SDCT).
- The proposed methodology is obtained from the data of actual damaged tunnels from past reported earthquakes. The database used is the global largest, as it contains 235 damaged tunnel information from 26 earthquakes.
- This simplistic method can identify the seismic vulnerability of rock tunnels (SVRT) before an earthquake.
- The proposed methodology does not require complex mathematical calculations and modeling, as it can be used by engineers for preliminary investigations.

Abbreviations

SDCT	Seismic damage classification of tunnels
SDDT	Seismic damage database of tunnels
SVRT	Seismic vulnerability of rock tunnels
DI	Damage Index
RMR	Rock mass rating
GSI	Geological Strength Index
Q	Rock mass quality of Q system
JH	Japanese highway rock mass classification
BQ	Engineering rock mass basic quality classification of Chinese national standard
M_w	Moment magnitude
GMPE	Ground motion prediction equations
PGA	Peak ground acceleration
PHA	Peak horizontal acceleration
R_{rup}	Minimum distance to the rupture surface
R_{hypo}	Hypocentral distance
SSD	Source-to-site distance
PSD	Potential secondary damages
PGV	Peak ground velocity
OD	Overburden depth
EH	Extremely high
VH	Very high
H	High
M	Moderate
L	Low
VL	Very low
EL	Extremely low

1 Introduction

The rock tunnels play a prominent role in modern-age infrastructures. Most of the rock tunnels are constructed in a hilly region, as they provide the shortest motorable link between two places. The rock tunnels residing in a seismic zone are considered safe and resistant to earthquakes. However, numerous earthquakes such as the Kobe, Chi-Chi, Wenchuan, and many more earthquakes showed that rock tunnels also are vulnerable to seismic damage (Wang et al. 2001; Wang and Zhang 2013; Yu et al. 2016a). Therefore, addressing the vulnerability caused by rock tunnels due to earthquakes is important. The damage degree and damage classification are prominent components of understanding the seismic vulnerability of rock tunnels (SVRT). Numerous researchers such as Dowding and Rozen (1978) categorized seismic damage for 71 cases of rock tunnels. Later, Owen and Scholl (1981) and Sharma and Judd (1991) updated the work of Dowding and Rozen (1978) by adding several cases to their database which consists of 127 and 192 cases of underground structures, respectively. Wang et al. (2001) has given a classification with a description for each class which was based on the functionality after the earthquake, length, width of cracks, and other damages to a tunnel. Yashiro et al. (2007) and Jiang et al. (2010) modified Asakura and Sato's (1996) classification for the tunnels damaged due to Mid-Niigata Prefecture. Due to the severe damage caused to tunnels by the Wenchuan earthquake, Wang's et al. (2001) classification was modified by researchers (Wang and Zhang 2013; Shen et al. 2014; Yu et al. 2016b) by adding the collapse or extremely severe damage level. Shrestha et al. (2020) further modified Wang's et al. (2001) classification and damage description as the damage due to the Gorkha earthquake was not so severe in the Melamchi tunnel. Xu et al. (2021) also provided a damage description for five damage levels. All these are post-seismic damage classifications. They provide a limited damage description for each proposed damage level and can't be used before an earthquake event.

Various researchers (Corigliano et al. 2007; Argyroudis and Pitilakis 2012; Qiu et al. 2018; Nguyen et al. 2019) worked on damage states and deriving Damage Index (DI) of tunnels based on seismic fragility curves. These curves represent the conditional probability of exceeding a predefined damage state as a function of a given intensity measure of ground motion (Nguyen et al. 2019). The DI is defined as the ratio between the actual bending moment (M) and capacity bending moment (M_{Rd}) of the tunnel cross section (Argyroudis and Pitilakis 2012). The empirical fragility curves for rock and cut-and-cover tunnels are adopted from reports of Dowding and Rozen (1978), and Owen and Scholl (1981). These empirical curves have limitations such as not considering specific factors like geological and structural characteristics of the tunnel adequately (Nguyen et al. 2019). It needs a large amount of damage database of past earthquakes, for empirical fragility curves to be statistically meaningful (Nguyen et al. 2019). Due to these limitations, the numerical fragility curves are widely used and a series of fragility curves are developed for bored circular tunnels. However, numerical fragility curves will inherently be limited by the constraints of numerical modeling, such as accurately representing the physical characteristics of geology. Regarding the damage states (Qiu et al. 2018), the four damage levels minor, moderate, extensive, and collapse are used to describe the damage which is based on classification studies of Wang et al. (2001), Yashiro et al. (2007), and Wang and Zhang (2013). A mathematical formulation-based seismic tunnel damage prediction model was given by Ansari et al. (2023) using the deep neural learning approach, which

is a type of machine learning. Furthermore, the proposed damage states are based on DI. The equation of DI proposed by Ansari et al. (2023) from the machine learning algorithm provides the range of DI between 3.1 and 3.5 for all the practical input values. Hence, the proposed equation classifies only minor damage levels for all the tunnels. Their validation is based on R^2 (coefficient of determination), which should not be the suitable parameter if the data used for validation comprises majorly minor damage cases. Deep learning platforms used in pattern recognition and classification should be supported by very large data sets (Lu et al. 2018). Using AI/ML techniques on limited data is not appropriate, which limits the applicability of such tools in seismic damage prediction models for tunnels.

It is concluded that the existing damage classifications are based on post-seismic damage investigations. The seismic damage prediction method proposed by Ansari et al. (2023) predicts only minor damage. The damage degree and damage descriptions in the post-seismic damage classifications were modified by researchers based on the amount of damage caused to a tunnel. These damage descriptions in classifications lacked a relation with influence parameters, were not uniform, and were specific to one or at a maximum of three seismic events. Above all, the databases utilized by researchers (Dowding and Rozen 1978; Owen and Scholl 1981; Sharma and Judd 1991; Asakura and Sato 1996; Jiang et al. 2010; Wang and Zhang 2013; Shen et al. 2014; Yu et al. 2016b) for assessing the damage also contain a major percentage of undamaged cases. These post-seismic classifications were modified for every seismic event, were not

Fig. 1 List of 26 major earthquakes included in SDDT that damaged 235 rock tunnels
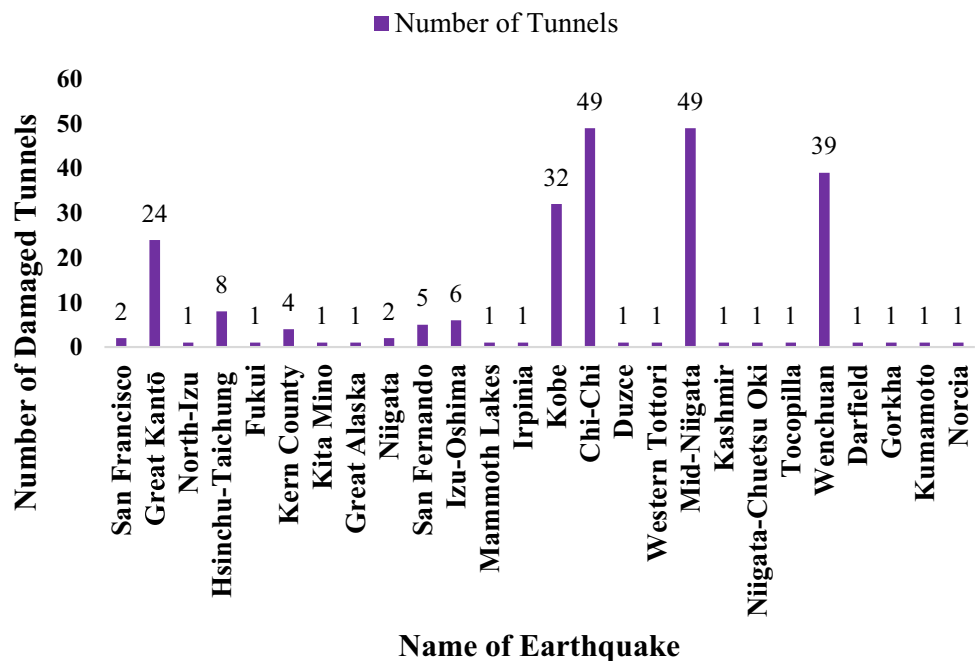
uniform, and lacked the amount of data. To obtain uniformity and consistency in the damage classification, the amount of data required is large. To assess the seismic damage to tunnels, the data should not be confined to a single or few seismic events in a particular region. To overcome the above limitations, this study aims to establish a simplistic method to predict and assess the seismic damage to the rock tunnels using seismic damage classification of tunnels (SDCT) before an earthquake. This study introduces three key aspects. First, the proposed SDCT is obtained by creating the largest global seismic damage database of tunnels (SDDT) which uses actual damage data from 235 damaged tunnel sites from 26 different earthquakes. These 26 earthquakes include the oldest 1906 San Francisco to the recent 2016 Norcia earthquakes. The number of damaged tunnels utilized in creating an SDDT due to respective earthquakes is shown in Fig. 1. Utilizing SDCT, this study proposes seven damage classes from extremely high (EH) to extremely low (EL). Each damage class has damage categories with detailed descriptions and are also linked to influence parameters. Second, from the proposed SDCT, a critical combination of influence parameters that affect the rock tunnels during earthquakes is identified and detailed in each class. Third, a simplistic and straightforward approach is suggested, relying on the critical combination of seven factors to assess the SVRT before an earthquake. This method simplifies the differentiation of seismic, geological, and structural factors in each damage class, facilitating predictions of potential damage levels at the site. It aids engineers to develop the seismic parameters initially and understand the seismic environment of the site. With seismic parameters in place, engineers can effectively assess damages using geological and structural factors of the site.

The proposed methodology is based on the largest database created so far, can be used prior to the earthquake, and is simple to use, without the need for intricate mathematical computations or modeling. This simplistic methodology serves as a valuable tool for preliminary assessments by engineers. The uniqueness of this classification and methodology lies in the simplicity for engineers to utilize it in the field for predicting damage in rock tunnels residing in the seismic zone. The validation of this study is done for Erkenek tunnel damage due to the 2023 Pazarcık, Kahramanmaraş earthquakes of Türkiye. This article is considered as part 1. In this article, Sects. 2, 3, and 4 describe SDDT, proposed SDCT, and methodology for seismic damage prediction along with a validation from the data of the Türkiye earthquake of 2023 followed by discussion and conclusion. This article has a follow-up as part 2, which utilizes the classification and methodology of this study. A software is developed employing the proposed methodology of this paper. This software is the outcome of a Python-based GUI tool. This tool is developed
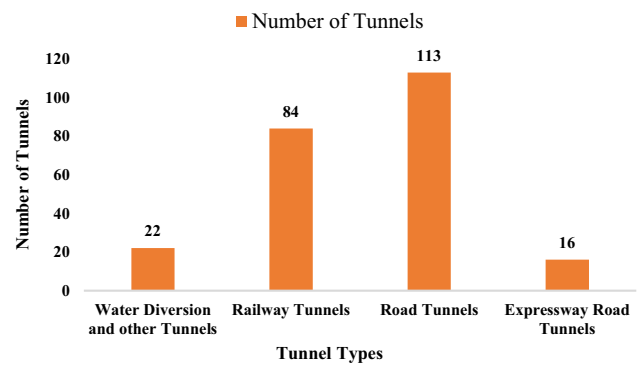

Fig. 2 Distribution of tunnel types considered in SDDT

based on data from seismic sources in India and adjacent countries. These sources act as input data for the written Python code. The code is designed to identify seismic sources within 250 km of a given location (latitude and longitude), the user enters. It then calculates and provides the distances from the site to each of these sources. The moment magnitude (M_w) of each fault is obtained through empirical correlations between M_w and the length of the fault surface. The peak ground acceleration (PGA) is also obtained for each source by utilizing the empirical attenuation relationship. For SVRT, parameters are latitude and longitude of the tunnel site, rock mass rating (RMR), overburden depth (OD), tunnel lining type, and tunnel shape. Critically combining all these parameters and obtained PGA, the software predicts the damage class and probable damages from seismic sources within the study region of a user. The reports are generated in.txt (notepad) format and include graphs for the distribution of total faults in each damage class. This tool enhances engineers' understanding of the SVRT before an earthquake in India and nearby countries.

2 Methodology for Data Collection and Creating SDDT

As an initial step for SDCT, the earthquake records that provide data on damaged tunnel sites are collected. A thorough literature survey is done for collecting the data and SDDT is created within MS Excel. A total of 235 rock tunnels damaged under 26 earthquakes consisting of road, expressway, railway, and water diversion tunnels are in SDDT. The distribution of each tunnel type is shown in Fig. 2.

The complete methodology adopted for creating an SDDT is shown in Fig. 3. In the SDDT, the influence parameters are categorized into structural, geological, and seismic parameters. The structural parameters like lining types and tunnel shape are obtained from various literature reports.
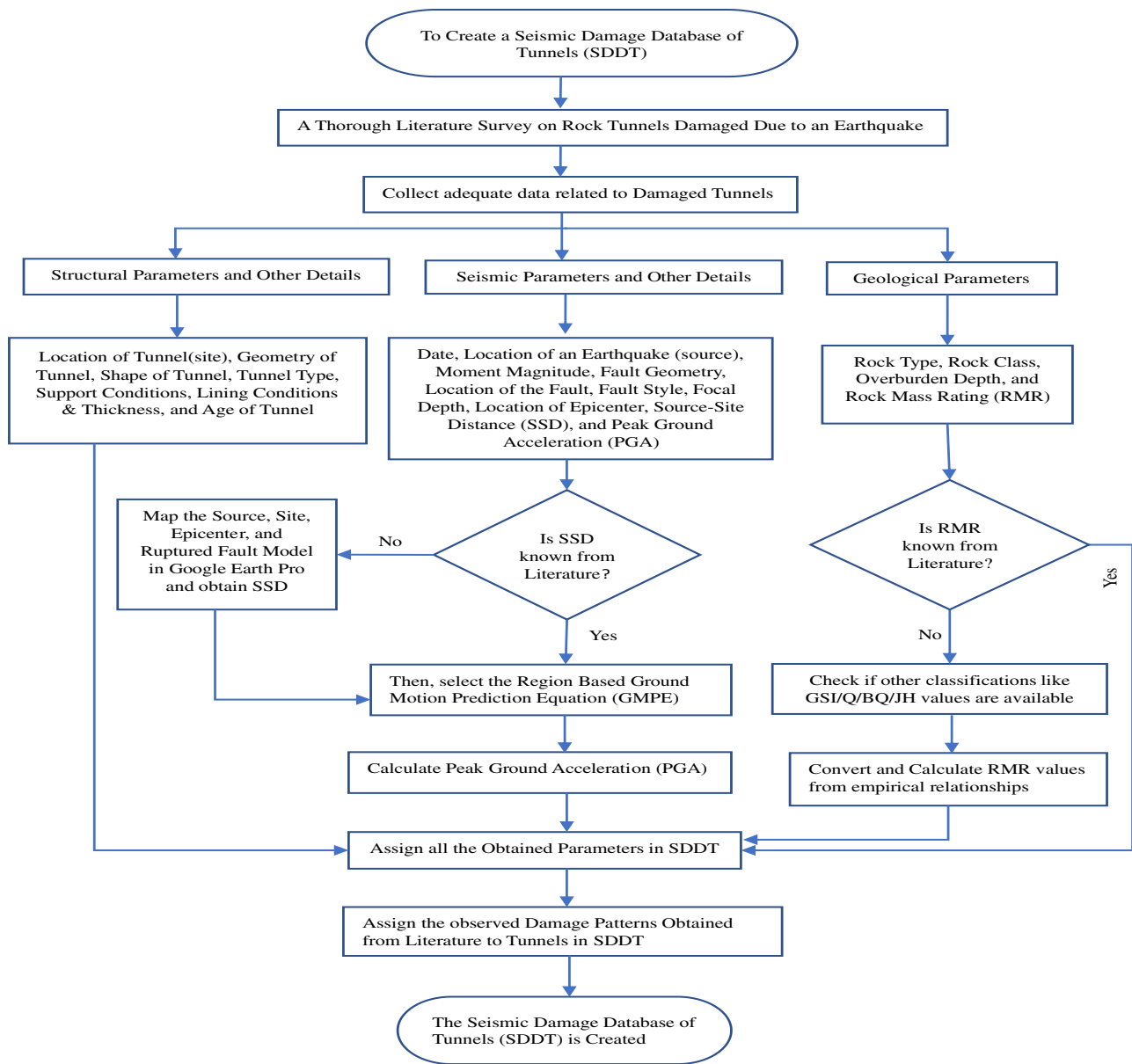
Fig. 3 Flowchart of the proposed methodology used to collect data and create an SDDT

Table 1 List of empirical equations used for obtaining RMR in this study

References	Parameters	Empirical equations	R^2
Hoek and Brown (1997)	GSI and RMR	$GSI = RMR'_{89} - 5$	–
Bieniawski (1993)	Q and RMR	$RMR = 9 \ln (Q) + 44$	0.77
Rahmati et al. (2014)	JH and RMR	$JH = 77.087 \ln (RMR) - 231.9$	0.88
Wu et al. (2023)	BQ and RMR	$BQ = 5.6755 RMR + 130.17$	0.63

The shape of the tunnels for a few cases is logged by obtaining and checking the images of tunnels through internet sources. To relate the damage with influence parameters, a comprehensive record of damages is also logged. The logging of geological, and seismic parameters and damages in SDDT are briefed in Sects. 2.1, 2.2, and 2.3.

2.1 Logging Geological Parameters in SDDT

The geological parameters considered in this study and logged in SDDT are rock class, RMR, and OD. Amongst the various rock mass classification systems, the RMR system is used as a major parameter in this study. This system is simple to use and is widely used in the field of tunneling (Bieniawski 1993). The RMR classification system divides rock masses into five classes: very good rock (RMR 81–100), good rock (RMR 61–80), fair rock (RMR 41–60), poor rock (RMR 21–40), and very poor rock (RMR < 20) (Bieniawski 1993). The RMR for a few tunnels in SDDT is directly obtained from the literature (Wang et al. 2001). If the RMR of the damaged tunnels is not available, but if other rock mass classification indices like Geological Strength Index (GSI) or rock mass quality (Q) system are available, the empirical relations for conversions such as GSI to RMR or Q to RMR are used as detailed in Fig. 3. For a few tunnels where the data is not available, an attempt is made to obtain GSI ranges visually through the pictorial representations of damaged tunnel sites with the rock mass around the tunnel. GSI is obtained by choosing the category based on geological descriptions given by Hoek and Brown (1997). The empirical relations for obtaining RMR are given in Table 1.

The Japanese highway (JH) rock mass classification is used to classify the rock mass and to obtain an adequate support system for the tunnels in Japan (Shinji et al. 2002). The range of the JH system is from 0 to 100. This System is based on intact rock material strength, weathering, joint spacing, and joint condition. The rock classes are divided into B-a, CI-a, CII-b, DI-a, DI-b, and DIII-a for respective JH values. The rock mass classes have varying JH values for different rock categories such as soft, med-hard, med-hard to soft, hard, and all rock types. To obtain the JH value for a few damaged tunnels in Japan, this study utilized the rock category of all rock types. The study of Rahmati et al. (2014) gives insight into RMR and JH relations given in Table 1.

For the tunnels affected due to the Wenchuan earthquake, the geology condition is categorized as soft rock or hard rock (Shen et al. 2014) and there was little information about rock mass and classification. Therefore, field data of damaged tunnels from the Du-Wen expressway and Guang-Gan expressway were collected from the studies of Cui et al. (2021). Data collected from the Du-Wen expressway

and Guang-Gan expressway were generalized as the hard rock mass and soft rock mass data, respectively (Cui et al. 2021). This field data is in the form of an engineering rock mass basic quality index (BQ) system, which is the Chinese national standard for the engineering classification of a rock mass. It is based on quantitative indexes, i.e., the saturated intact uniaxial compressive strength (Rc), intactness index of the rock mass (Kv), and the correction coefficients for groundwater correction K1, joint orientation to the excavation K2 and in-situ stress coefficient K3. The BQ system divides all rock masses into five classes and the rating is given as > 550 for class 1 to ≤ 250 for class 5. The study of Wu et al. (2023) gives insight into RMR and BQ relations. The empirical relation with their coefficient of determination (R^2) is given in Table 1. To classify the rock mass around these tunnels, the geology conditions provided by Shen et al. (2014), field studies of Cui et al. (2021), and the empirical relations of Wu et al. (2023) are combined, categorized, calculated, and logged into this database.

Despite the coefficient of determination (in Table 1) being 0.77 and 0.63 for Q to RMR and BQ to RMR relations, they are used in this study. This is because the Q to RMR relation in Table 1 is widely used and the BQ to RMR relation in Table 1 is the most recent established study. The RMR is unknown for a few tunnels constructed before the existence of rock mass classifications. For such tunnels, the available descriptions of rock mass and type are used to obtain the RMR. The descriptions of various sites encountered in the SDDT are bought together for allotting the RMR as detailed in Table 2. Thus, utilizing all the parameters and empirical relationships, the RMR is obtained and logged into the database.

2.2 Logging Seismic Parameters in SDDT

This study utilizes moment magnitude (M_w) as a magnitude scale and for the first time, region-based attenuation relationships are selected for obtaining PGA for 26 earthquakes. This contrasts with previous studies (Dowding and Rozen 1978; Sharma and Judd 1991; Roy and Sarkar 2017), which obtained PGA using a single common attenuation relationship for worldwide tunnels in their database. The region-based attenuation relationships provide a realistic PGA value at sites. Table 3 provides complete information

Table 2 RMR ranges in SDDT utilizing a description of rock type and rock mass

Description of rock type and rock mass	RMR
Known and unknown rock type/s mentioned as soft rock (softer strata)	15.0–40.0
Known and unknown rock type/s are mentioned as soft rock with rock class "Very Poor"(softer strata and fault fracture zones)	15.0–25.0
Known and unknown "Fair" rock type/s are mentioned as hard rock in the description	40.0–60.0
A known rock type mentioned as hard rock with a rock class is "Good"	61.0–80.0

Table 3 Details of seismic events and GMPE utilized for this study

S. no.	EQ name/M_w	Year of EQ	GMPE [ref]	Location for GMPE application	Range of M_w	Distance range (in km)	Damaged tunnel cases
1	San Francisco/7.9	1906	[1]	California	4–8+	≤100	2
2	Great Kanto/7.9	1923	[2]	Japan	≥5.5	≤425	24
3	North-Izu/7.1	1930	[2]	Japan	≥5.5	≤425	1
4	Hsinchu-Taichung/7.1	1935	[3]	Taiwan	5.3–8.1	15–630	8
5	Fukui/6.8	1948	[2]	Japan	≥5.5	≤425	1
6	Kern County/7.3	1952	[1]	California	4–8+	≤100	4
7	Kita Mino/6.8	1961	[2]	Japan	≥5.5	≤425	1
8	Alaska/9.2	1964	[4]	Worldwide	≥5	10–500	1
9	Niigata/7.6	1964	[2]	Japan	≥5.5	≤425	2
10	San Fernando/6.6	1971	[1]	California	4–8+	≤100	5
11	Izu Oshima/6.6	1978	[2]	Japan	≥5.5	≤425	6
12	Mammoth Lakes/6.2	1980	[1]	California	4–8+	≤100	1
13	Irpinia/6.9	1980	[10]	Italy	4.0–7.5 (M*)	0–200	1
14	Kobe/6.9	1995	[2]	Japan	≥5.5	≤425	32
15	Chi Chi/7.6	1999	[5]	Taiwan	3.5–7.6	1–240	49
16	Duzce/7.2	1999	[11]	Northwestern Türkiye	5–7.5	0–200	1
17	Western Tottori/6.6	2000	[2]	Japan	≥5.5	≤425	1
18	Mid-Niigata prefecture/6.6	2004	[2]	Japan	≥5.5	≤425	49
19	Kashmir/7.6	2005	[6]	Worldwide	4–8.5	0–200	1
20	Niigata-ChuetsuOki/6.6	2007	[2]	Japan	≥5.5	≤425	1
21	Tocopilla/7.7	2007	[4]	Worldwide	≥5	10–500	1
22	Wenchuan/7.9	2008	[7]	Southwest China	4.2–7.9	0–300	39
23	Darfield/7.1	2010	[8]	New Zealand	4.5–8.5	0–100	1
24	Gorkha/7.8	2014	[9]	North and Central Himalayas	4.1–7.8	1560	1
25	Kumamoto/7.0	2016	[2]	Japan	≥5.5	≤425	1
26	Norcia/6.6	2016	[10]	Italy	4.0–7.5 (M*)	0–200	1

Remarks: EQ—earthquake, M_w—moment magnitude, (*) M_s: surface wave magnitude, GMPE—ground motion prediction equation, [ref]—references

[1] Sadigh et al. (1997), [2] Kanno et al. (2006), [3] Lin and Lee (2008), [4] Youngs et al. (1997), [5] Lin et al. (2011), [6] Campbell and Bozorgnia (2008), [7] Zhang et al. (2022), [8] Bradley (2013), [9] Ramakrishnan et al. (2021), [10] Montaldo et al. (2005), [11] Özbey et al. (2004)

on 26 earthquakes in SDDT. It includes name, year, M_w, ground motion prediction equations (GMPE) used for each earthquake, and GMPE details like applicability of location, magnitude and distance ranges, and number of tunnels analyzed through respective GMPE.

2.2.1 The Selection of Attenuation Relationships

From attenuation relationships, the upper bound peak horizontal acceleration (PHA) values for rock sites are considered in this study. The vertical seismic motion is considered to have a minor effect on the seismic response of the tunnel (Yu et al. 2016a). Therefore, it is neglected for seismic design (Yu et al. 2016a). Calculated PHA is referred to as PGA in this article from hereon. The GMPE of the attenuation relationships used in the study is not provided in this

paper, but appropriate references are mentioned in Table 3. The GMPE of Sadigh et al. (1997) is used for the tunnels damaged due to earthquakes in rows 1, 6, 10, and 12 of Table 3, as it is based primarily on data from California earthquakes. For the tunnels affected from Great Alaskan (1964) and Tocopilla (2007) subduction zone earthquakes (rows 8 and 21 of Table 3), the attenuation relationship of Youngs et al. (1997) is used as it is the relationship for subduction zone earthquakes. Although this relationship is applicable worldwide, their study consists of major data from subduction zone earthquakes of Alaska and Chile.

For Japanese tunnels damaged due to various earthquakes, (rows 2, 3, 5, 7, 9, 11, 14, 17, 18, 20, and 25 of Table 3) the attenuation relationship of Kanno et al. (2006) is used as it contains one of the largest strong ground motion records of Japan. Although the applicability of

Kanno et al. (2006) relationship is worldwide, their study consists of major data from Japan. For the damaged tunnel sites due to the 1935 Hsinchu-Taichung and 1999 Chi-Chi earthquakes, the attenuation relationships of Lin and Lee (2008) and Lin et al. (2011) are used as they are specifically based on the strong ground motion records of North-Eastern Taiwan and Taiwan, respectively. For the tunnel damage due to the 1999 Duzce earthquake, the GMPE of Özbey et al. (2004) is used as it is specific to recordings of North-Western Türkiye. Since no region-specific GMPE model is available for Pakistan (Hashash et al. 2012), this study used Campbell and Bozorgnia's (2008) relationship for tunnel damage due to the 2005 Kashmir earthquake.

For the tunnels affected due to the 2008 Wenchuan and 2010 Darfield earthquakes, Zhang et al. (2022) and Bradley's (2013) attenuation relationships are used, respectively. They are specifically based on a data set of earthquakes in Southwest China and New Zealand, respectively. For the tunnels damaged due to the 1980 Irpinia and 2016 Norcia earthquakes, the GMPE of Montaldo et al. (2005) is used as it is based on Italian strong-motion data. For the damaged tunnel site due to the Gorkha earthquake, the attenuation relationship of Ramakrishnan et al. (2021) is used as it is based on strong motion data of the North and Central Himalayas.

2.2.2 The Evaluation of PGA

For obtaining PGA, the minimum distance to the rupture surface (R_{rup}) or the Hypocentral distance (R_{hypo}) is used as source-to-site distance (SSD). If the rupture surface was not defined for an event, then R_{hypo} is used as the SSD (Sadigh et al. 1997; Youngs et al. 1997; Kanno et al. 2006). The use of R_{hypo} does not introduce significant bias in the attenuation models. The SSD is obtained directly for a few tunnels from the literature (Rozen 1977; Jiang et al. 2010). For the tunnels

affected by Chi-Chi, R_{rup} is given in the literature (Wang et al. 2001). If the SSD is not available directly, the ruptured fault and tunnel site are mapped in Google Earth Pro for respective seismic events. The data on ruptured faults are obtained from databases like the FDHI database (Sarmiento et al. 2021). The location of the tunnel and the ruptured fault plane are mapped in Google Earth Pro and a distance indicator tool is used to obtain the SSD. If the rupture fault plane is not available, the epicenter and tunnel site are mapped and the focal depth of the event is utilized for obtaining R_{hypo}. Thus, various approaches as mentioned above are used to obtain SSD for calculating the PGA.

2.3 Logging the Damage Patterns in SDDT

The reported seismic damages are named in numerous ways in literature sources. Utilizing the literature sources, the initial step is to log the actual seismic damages to the rock tunnel sites from seismic events. The damage patterns in the 235 rock tunnels varied from tunnel collapse and secondary damages such as spalling, deformation, and rock fall, to minor cracks. This concludes the creation of SDDT with all the required parameters. The details of 235 rock tunnels considered in the SDDT are provided in Annexure A of Supplementary Material. The proposed classification utilizing SDDT is elaborated in Sect. 3.

3 Seismic Damage Classification of Tunnels (SDCT)

From SDDT, the various damage patterns incurred in tunnels are brought together to classify and understand the damage characteristics. It is observed that seismic damage to the tunnel is divided based on damages incurred in a tunnel at three locations namely lining, portal, and invert. Utilizing the damage patterns and amount of damage from 235 tunnels of SDDT, the classification based on lining, portal, and
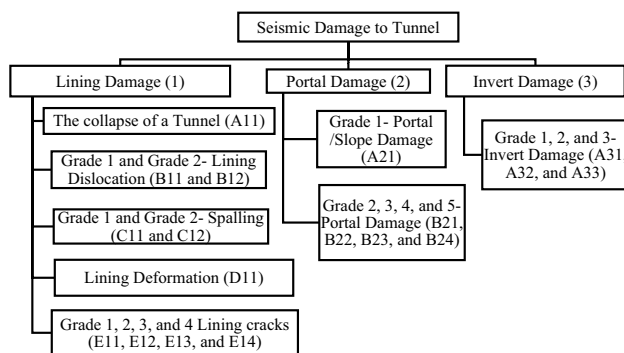
Fig. 4 Organization chart of seismic damage classification of tunnels (SDCT)

Table 4 Damage classes and categories from cases in SDDT

Damage class	Damage categories	No. of tunnel cases
Extremely high (EH)	A11	3
Very high (VH)	B11, A21, A31	23, 14,11
High (H)	B12, C11, E11, B21, A32	6, 10, 7, 10, 4
Moderate (M)	C12, D11, E12, B22, A33	47, 25, 48,18,14
Low (L)	E13, B23	7, 7
Very low (VL)	E14, B24	11, 4
Extremely low (EL)	N*	0

Remarks: N* is no damage scenario

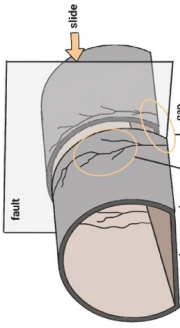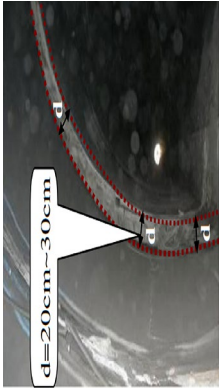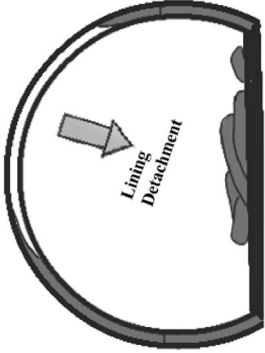**Table 5** Description of various damage categories in seismic damage classification of tunnels (SDCT)

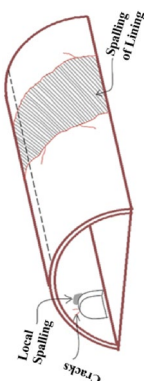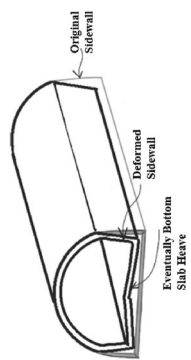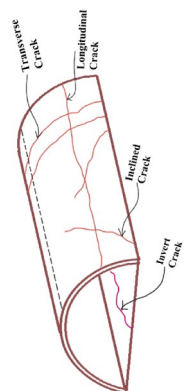| Damage	Damage definition	Appearance of damage	PSD	Amount of damage	Case histories*/Ex.**	Comments
[1] The collapse of a tunnel body (A11)—(EH)	The collapse of a tunnel body or sheared-off lining is caused by shear stress in the tunnel, usually occurring in tunnels that intersect with ruptured faults		B11 B21 A21 A31 C11 D11 E11	(a) Tunnels intersecting the faults are sheared off or dislocated up to 3–4 m vertically and horizontally (b) Major sections of lining or roof cave in and completely fall and collapse (c) Will lead to a collapse of a tunnel	3 cases/Tanna, Shih-Gang, and the Inatori tunnels	Among all the grades, this is the higher form of damage
[2] Grade 1—lining dislocation (B11)–(VH)	Caused by shear stress in the tunnel, occurring in tunnels very close to ruptured faults (≤5 km)		B21 A21 A31 C11 D11 E11	(a) Lining is sheared off or dislocated up to 2 m vertically and horizontally (b) A section of lining or roof caves in and completely falls and collapses (c) Will either lead to collapse or heavy rehabilitation of the tunnel	23 cases/Wright -1, S.P.R.R. 3, 4, 5, 6 tunnels, Longxi, Zipingpu, Baiyunding tunnels	(a) Differentiated from the above case based on PGA, SSD, and the amount of damage (b) Also contains a few tunnels which are collapsed
[3] Grade 2—lining dislocation (B12)–(H)	Caused by shear stress in the tunnel, occurring in tunnels close to ruptured faults (3–15 km)		C12 E12 A33	(a) Lining is dislocated up to 0.8 m horizontally and slightly shifted vertically (b) A portion of the roof caves in and falls (c) Will lead to heavy rehabilitation of the tunnel	6 cases/Tottori Head race, Komine, Ippamatzu Tunnels	(a) The amount of damage and PSD for the B12 case is lesser compared to B11 and A11 (b) Tunnel will not collapse but it is damaged badly
[4] Grade 1—lining spalling (C11)–(H)	This results from compression force along the direction of the tunnel axis. The seismic shaking force is the initiation factor for spalling		E13 E14	(a) A large-scale spalling characterized by the detachment of lining or steel reinforcements, severe falling of lining, exposed Reinforcement, distortion, and surrounding rock collapse (b) Area of crushed lining is> 2 m^2 (c) Requires heavy rehabilitation of the tunnel	10 cases/Izu-Kitagawa, Maanshi Panlongshan tunnels	Also characterized by a slight portion of rock chunks falling in the tunnel

Table 5 (continued)

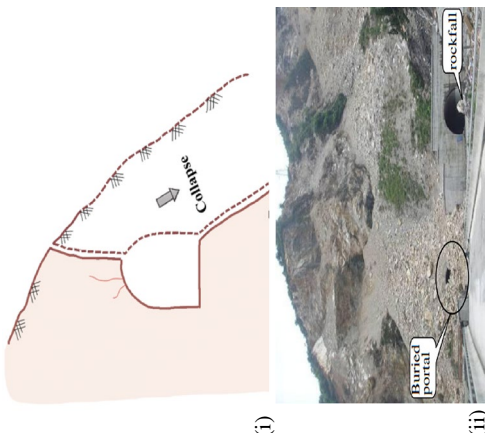| Damage	Damage definition	Appearance of damage	PSD	Amount of damage	Case histories*/Ex**	Comments
[5] Grade 2—lining spalling (C12)–(M)	Same as C11		E14	(a) A small-scale spalling characterized by the detachment of lining or steel reinforcements, moderate to slight falling of lining, and exposed reinforcement (b) Area of crushed lining is <2 m^2 (c) Requires moderate rehabilitation of the tunnel	47 cases/ Melamchi, Shin-Kobe, Haneguro (pavement) tunnels	(a) PSD for this case is just minor lining cracks or no PSD at all (b) Amount of damage and PSD for the C12 is lesser compared to C11
[6] Lining deformation (D11)–(M)	(a) Characterized by deformed lining or lateral shift in the lining (b) Caused by significant inward deformation of the sidewalls and sometimes the tunnel crown		C12 E14 A33	(a) The lining is deformed up to a maximum of 25 cm horizontally (b) The Crown and sidewall of the tunnel are deformed or laterally shifted sideways from the original position (c) Requires moderate rehabilitation of the tunnel	25 cases/No. 1 San-I railway, Kizawa, Wanantu (road and railway), San Benedetto tunnels, and others	This case will also cause slight upheaval at the tunnel bottom due to compression from sidewalls
[7] Grade-1, 2, 3, and 4 lining cracks (E11, E12, E13, and E14)–(H, M, L, and VL)	When axial stress (compression or tension) along the tunnel extension direction exceeds the corresponding (tensile or compression) strength of the lining concrete, cracks will initiate and develop		B23 B24	(a) E11: cracks extend up to $1>15$ m, $w>35$ mm (b) E12: cracks extend up to l: 5–15 m, w: 5–35 mm (c) E13: cracks extend up to $1<5$ m, $w<5$ mm (d) E14: cracks extend up to $1<1$ m, $w<3$ mm (e) Requires just a slight rehabilitation of the tunnel	7, 48, 7, and 11 cases, respectively /E11, E12, E13 and E14-Tou-6 highway, Suma, Lyttelton Road, and Mafu tunnels, respectively	Minimal and most frequent types of seismic damage to tunnels. Can be further classified as inclined, longitudinal and transverse crack

Table 5 (continued)

Damage	Damage definition	Appearance of damage	PSD	Amount of damage	Case histories*/Ex**	Comments
[8] Grade-1 Portal/slope damage (A21)–(VH)	(a) Portal sections are the most vulnerable part of the tunnel (b) This case usually occurs in tunnels very close to ruptured faults (≤5 km) (c) Slope failure-induced tunnel collapse is also part of this case as shown in (i) of the appearance column	(i) (ii)	B11 A31 C11 E11	(a) Characterized by portal/slope collapse, head wall fractured by heavy rockfalls, and completely buried tunnel portal (b) Will lead to either collapse or heavy rehabilitation of the tunnel	15 cases/Highway 149, Ching-Shue tunnel, Hakone-3, Hakone-4, Happon Matsu, and Longdongzi tunnels	Tunnels will undergo any combination or will undergo all the damages mentioned in the amount of damage column
[9] Grade-2 portal damage (B21)–(H)	(a) Caused due to seismic inertia force or surrounding rock instability alongside activities like rockfall or slope failure (b) The forced deformation between the structure and strata leads to portal damage at a weak zone of a rock mass		C12 E12	(a) Characterized by severe failure of a slope and rock fall, most part of the tunnel portal is buried, and portal wall cracking (b) Severe damage to the portal such as loosening of the curved head-wall of the portal, and structure puncture (c) Requires heavy rehabilitation of the tunnel	10 cases/Hichigama tunnel, Kanome-Yama, Ajo, and Maanshi tunnels	Same as A21

Table 5 (continued)
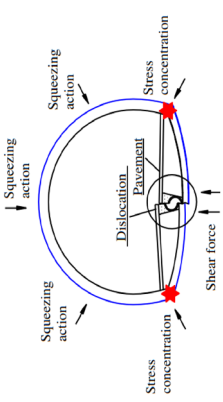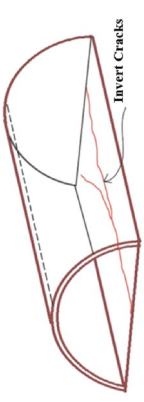
Damage	Damage definition	Appearance of damage	PSD	Amount of damage	Case histories*/Ex**	Comments
[10] Grade-3 portal damage (B22)—(M)	Same as B21		C12 E12	(a) Characterized by moderate rock fall, massive gravel, or large stones piled up/overlaying of rock and soil deposits in front of a portal, and portal cracks of continuous ring-shaped ($w > 15$ mm) (c) Requires moderate rehabilitation of the tunnel	18 cases/ Hamuya, Chediguan, and Yinxing tunnels	Same as A21
[11] Grade-4 portal damage (B23)—(L)	Same as B21		E13 E14	(a) Characterized by small-scale rock fall, sparse gravel, or small stones piled up in front of a tunnel, and portal cracks ($w < 15$ mm) (b) Requires just a slight rehabilitation of the tunnel	7 cases/Caopo, Dankanliangzi, and Fenshuiling tunnels	(a) PSD for this case is just lining cracks or no PSD at all (b) The amount of damage and PSD for the B23 case is lesser compared to B21 and B22
[12] Grade-5 portal damage (B24)—(VL)	Among all the grades of portal damage, this is the minimal form of damage		E14	(a) Characterized by overhead raveling of loose rock that will fall on a tunnel or slight chipping of rock chunks from a slope or slight cracks in the portal (b) Requires slight rehabilitation of the tunnel	4 cases/Whittier Tunnel, Helms Project Tunnel, Mingyuexia, and Feixianguan Tunnels	PSD in this case is just cracks in the lining or no PSD at all
[13] Grade 1—invert damage (A31)—(VH)	The Shear force concentration at the bottom of the tunnel and stiffness mismatch between different materials are observed to be the main causes of invert damage		B21 A21 C11 D11 E11	(a) Characterized by severe invert upheaval ($h_u < 150$ cm), severe extended cracks ($l \geq 20$ m, $w \geq 10$ cm) at the tunnel bottom, and invert will dislocate laterally (b) Will lead to either collapse or heavy reinforcement of the tunnel	11 cases/ Pavoncelli, Tawarayama, Longxi, Shaohuoping, and Zipingpu tunnels	The higher form of Invert damage

Table 5 (continued)

Damage	Damage definition	Appearance of damage	PSD	Amount of damage	Case histories*/Ex**	Comments
[14] Grade 2—invert damage (A32)—(H)	Same as A31		D11 E13 B23	(a) Characterized by moderate invert upheaval (h_u <50 cm) and moderate-scale cracks (1<20 m, w<10 cm) at the tunnel bottom (b) Requires heavy rehabilitation of the tunnel	4 cases/ Jiujiaya, Maanshi, and Ippamatzu tunnels	This case will be associated with deformation in the sidewalls of tunnels
[15] Grade 3—invert damage (A33)—(M)	Same as A31		C12 E13 B23	(a) Characterized by slight invert upheaval (h_u <20 cm) or slight cracks (1<5 m, w<5 cm) at the tunnel bottom (b) It requires moderate rehabilitation of the tunnel	14 cases/ Rokko, Bantaki, Haneguro, and Hosa tunnels	PSD and amount of damage for the A33 case are lesser compared to A31 and A32

Remarks: PSD—potential secondary damages, case histories*—number of damaged cases in each damage type, Ex**—few examples of case histories, Title of figures are same as mentioned in column 1 of 'Damage'; The sources of figures are mentioned in order of serial number [1–15] as: [1, 5, 6, 8(a), 15] Wang et al. (2001), [2, 3, 8(b), 9, 14] Shen et al. (2014), [4] Yashiro et al. (2007), [7] Roy and Sarkar (2017), [10] Wang et al. (2009), [11, 13] Li (2012), and [12] Asakura (1996). [2, 4, 5, 6, 7, 8a, and 15 are redrawn after mentioned sources], w–width of crack, l—length of crack, h_u—invert uplift height

invert damages is found to be uniform. The damage classification and its sub-categories are shown in Fig. 4. The damages to the lining, portal, and invert are categorized in order of the higher to the lower form of damage. For example, the collapse of a tunnel is the higher form. Minor damages like cracks are the least damage types as they are easily repaired. The moderate form of damage is accommodated in between these two forms. The lining damage is assigned with 1 and their sub-categories from A to E are given notations starting with 1. The higher form of lining damage is notated A11, followed by B11 and B12, C11 and C12, D11, and E11 to E14. The portal and invert damages and their sub-categories are notated starting with 2 and 3, respectively. For a Portal, A21 is the higher damage form followed by B21, B22, B23, and B24 being the lower, whereas A31 is the higher damage form for invert followed by A32 and A33 is lower.

To understand the damage levels caused in the tunnels, seven damage classes are introduced varying from extremely high (EH) to very low (VL) for damage categories as tabulated in Table 4. The extremely low (EL) class shows the negligible damage scenario. Table 4 also mentions the number of tunnel cases of respective damage categories for each damage class. This section elaborates on various damages and their categories. The detailing of a procedure for allotment of these classes linking to parameters is done in Sect. 3.1. All the damage categories mentioned in Table 4 and Fig. 4 are elaborated in Table 5 with their damage definition, appearance, potential secondary damages (PSD), amount of damage, and case histories considered in each category with some examples. If a tunnel is undergoing multiple damages, such as lining dislocation, lining spalling, and lining cracks, then the highest amount of damage incurred is considered as a damage category and the PSD is noted for every damage category. A few cases of lining damage will appear again in the portal and invert damage. This is because the tunnel might have undergone multiple damages due to seismic events. For example, a few cases of A21 and B11 are present in the A31. A31 is considered as the PSD of A21, B11, and vice versa. The amount of damage and PSD decreases for every level of damage class from EH to VL. It is to be noted that the damage definition and amount of damage in Table 5 are based on actual seismic damages of tunnels from literature sources (Dowding and Rozen 1978; Owen and Scholl 1981; Wang et al. 2001; Aydan et al. 2010; Wang and Zhang 2013; Shen et al. 2014; Yu et al. 2016b; Xu et al. 2021 amongst others).

From SDDT, the amount of damage is obtained for each category of lining, portal, and invert damages. The amount of damage is different for every tunnel in each category and it has either a physical damage description or also quantitative value for a few of the damage types. For example, the Longxi, Pavoncelli, and Zipingpu tunnels in the VH class have a maximum invert upheave height of 120, 150, and 60 cm, respectively. Therefore, for such cases, the maximum value of 150 cm is considered in the amount of damage for invert upheave height in the VH class. Similarly, it is allotted for other categories in each class. Therefore, the amount of damage assigned is based on the actual amount of damage that took place in the tunnels for each damage category.

In Table 5, for lining damage, the collapse, two grades of lining dislocation and spalling, and various grades of lining cracks are differentiated in detail. A separate category for lining deformation in side walls or arches is detailed. The Grade 1—portal/slope damage (A21)—is a single case of damage, as it also includes slope failure-induced tunnel collapse. Portal cracks, rockfalls, portal rupture, portal wall punctures, and headwall damage at the portal are bought together and accommodated into four different grades (B21–B24) of portal damage. In portal damage, portal cracks are not separated into different grades, whereas lining cracks in lining damage are separated into different grades. There are two reasons for not separating portal cracks into different grades. Most portal crack cases involve some degree of rock fall, and there are very few portal crack cases in SDDT. Three grades of invert damage are differentiated and there is no case of invert damage present in the L and VL damage classes.

3.1 The Analysis of SDCT

This SDCT is based on lining, portal, and invert damages in a tunnel. Generally, the seismic performance of the tunnel body (lining and invert) in a rock tunnel is highly influenced by seismic deformation and Peak Ground Velocity (PGV) should be a key parameter compared to PGA (Chen and Wei 2013). This is due to the confining effect of the surrounding ground on the tunnel body. For portals/slopes, PGA should be a key parameter in terms of the seismic capacity of the tunnel. The study of Huang et al. (2020) emphasized that it is important to take the PGA and PGV into account during seismic analysis and design for tunnels. However, this study considers PGA as a prominent parameter for the lining, portal, and invert of the tunnel combinedly. The main reason is, that the essence of obtaining PGA in this study lies in utilizing a region-based attenuation relationship. Most of the region-based attenuation relationships used in this study are commonly used for obtaining PGA and do not account for PGV at all (rows 1, 4, 6, 8, 10, 12, 13, 15, 16, 21, 23, 24, and 26 of Table 3). Hence, this study uses PGA values for all the cases.

3.1.1 Analysis of Influence Parameters: M_w, SSD, PGA, RMR, and OD from SDDT

From the SDDT, it was clear that collapse or extreme damage occurred when a rupture fault passed through or was
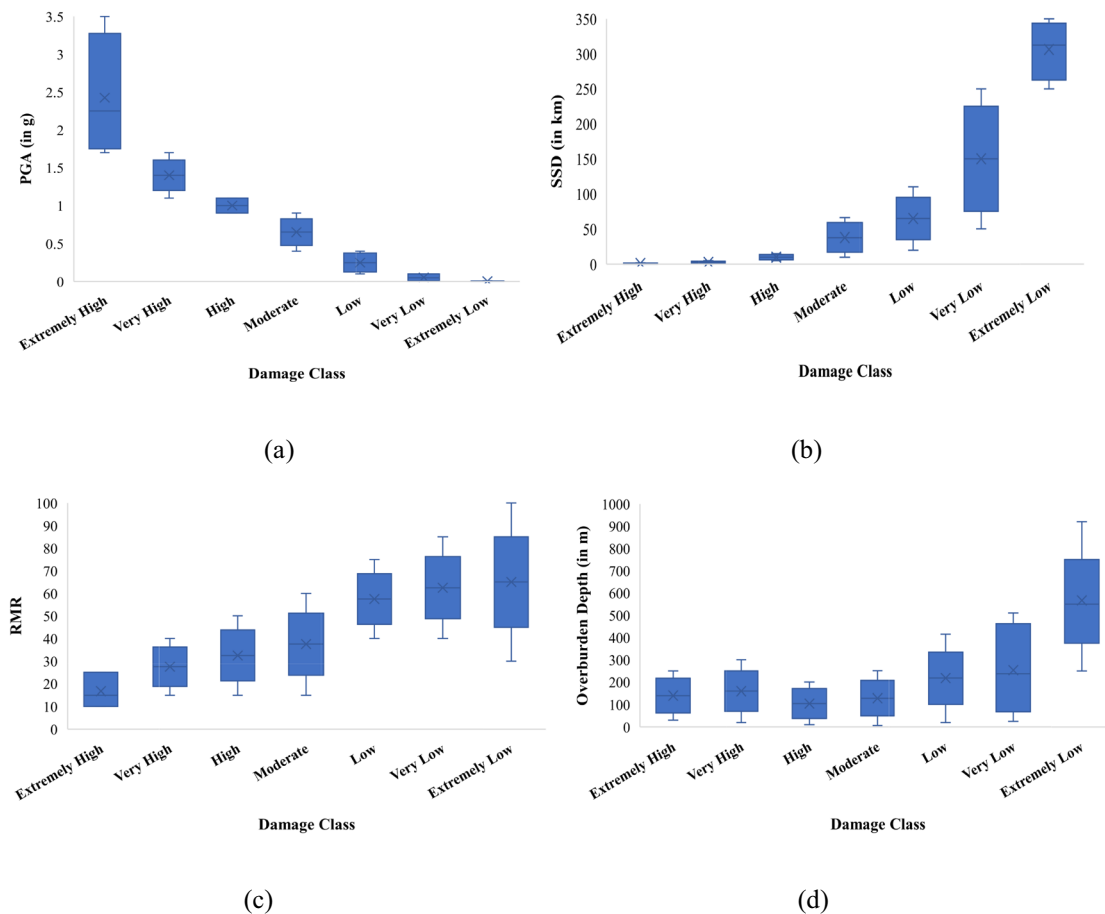
(a)

(b)

(c)

(d)

Fig. 5 Variation of damage classes with **a** PGA, **b** SSD, **c** RMR, **d** OD

close to the tunnel, indicating that SSD is very low. Conversely, when the rupture fault is far from the tunnel, SSD is higher. Generally, if SSD is low, the PGA is higher, and the observed amount of damage to tunnels in SDDT is more and vice versa. It is observed that the damage categories of this SDCT are well-fitted to certain ranges of SSD and PGA. The ranges of SSD and PGA are allocated after analyzing various cases for respective damage categories. For example, A11 and B11 are based on 3 and 23 cases, respectively. The tunnels in these 3 cases have higher PGA followed by tunnels in the 23 cases. This means A11 seems to have the higher PGA values (> 1.70 g) with SSD ≤ 2 km followed by B11 with PGA of 1.70–1.11 g and SSD ≤ 5 km. Similarly, other damage categories also seem to follow a certain range of PGA and SSD values as shown in Fig. 5a, b. Initially, based on PGA and SSD ranges, a damage class is allotted varying from EH to VL. It is to be noted that, these SSD and PGA conclusions are for M_w of 6.1–8 for EH, VH, H, M, and L classes and 6.1–9.2 for VL class.

Parameters such as the OD, RMR, lining type, and tunnel shape are identified as critical parameters alongside SSD and PGA in this study. For every damage class, the damaged cases are observed to identify the pattern of influence parameters. The identification of influence parameters for each damage class resulted in a critical combination of influence parameters. For example, B11, A21, and A31 have 23, 14, and 11 cases of damaged tunnels. For the B11, A21, and A31 categories, the PGA and SSD are known. Now for these categories, the RMR and OD are observed and a range is given based on those 23, 14, and 11 cases. Through this way, the B11, A21, and A31 categories of the very high (VH) class are allotted with obtained ranges of RMR, and OD from the SDDT. Therefore, for the VH class, the parameters M_w, SSD, PGA, RMR, and OD are known and the damages namely B11, A21, and A31 are known. This process is followed to the tunnels in SDDT for all the damage categories in each damage class. Through this process, the magnitudes of parameters related to each damage class were examined. It was observed that the ranges of SSD, RMR, and OD are lower at EH and VH classes and are higher at L and VL classes and vice versa for PGA, as shown in Fig. 5a–d. The complete quantitative ranges of each damage

Table 6 Criteria of probable seismic damages to the tunnel utilizing a critical combination of parameters

S. no.	Damage class	Parameters					Lining type (>)*	Shape (>)**	Probable damage			Accessibility of tunnel
		PGA (in g)	M_w*	SSD (in km)	RMR	OD (in m)			Lining	Slope/portal	Invert	
1	Extremely high (EH)	>1.70	6.1–8.0	≤2	10–25	30–250	UL>TL>ML>CL>RCL	RE>AH>D>HS>OV>CR	A11	–	–	AT1
2	Very high (VH)	1.70–1.11	6.1–8.0	≤5	14–40	20–300	UL>TL>ML>CL>RCL	RE>AH>D>HS>OV>CR	B11	A21	A31	AT1
3	High (H)	1.10–0.91	6.1–8.0	3–15	15–60	10–200	UL>TL>ML>CL>RCL	RE>AH>D>HS>OV>CR	B12, C11, E11	B21	A32	AT2
4	Moderate (M)	0.90–0.41	6.1–8.0	10–65	15–60	6–250	UL>TL>ML>CL>RCL	RE>AH>D>HS>OV>CR	C12, D11, E12	B22	A33	AT3
5	Low (L)	0.40–0.11	6.1–8.0	25–110	40–75	20–400	UL>TL>ML>CL>RCL	RE>AH>D>HS>OV>CR	E13	B23	N	AT4
6	Very low (VL)	0.10–0.01	6.1–9.2	60–250	40–85	20–500	UL>TL>ML>CL>RCL	RE>AH>D>HS>OV>CR	E14	B24	N	AT4
7	Extremely low (EL)	<0.01	6.1–9.2	>250	any	any	any	any	N	N	N	AT5

Remarks: M_w *—range of moment magnitude, PGA—peak ground acceleration (in g), SSD—source-to-site distance (in km), OD—overburden depth (in m), RMR—rock mass rating; (>)*—order of criticality for lining type of the tunnel, UL—unlined, TL—timber lined, ML—masonry lined tunnels (is either only brick or brick and stone work or brick and plain concrete), CL—concrete/reinforced concrete lined tunnels only with primary lining as major support, RCL—reinforced concrete lined tunnels with primary lining, secondary lining, and support system; (>)**—order of criticality for the shape of a tunnel, RE—rectangle, AH—arched with horizontal roof, D—D-shaped, HS—horse shoe, OV—ovoid, CR—circular. A11—the collapse of a tunnel; B11 and B12—Grade 1 and Grade 2—Lining dislocation, respectively; C11 and C12—Grade 1 and Grade 2—spalling, respectively; D11—lining deformation; E11, E12, E13, and E14—Grade 1, 2, 3, and 4 lining cracks, respectively; A21—grade 1—portal/slope damage; B21, B22, B23, and B24—Grade 2, 3, 4, and 5—portal/slope damage, respectively; A31, A32, and A33—Grade 1, 2, and 3—invert damage, respectively; N—no damage. AT1—tunnel cannot be operable after the seismic event; AT2—tunnel is operable after a seismic event with many precautions and caution boards; AT3— tunnel is operable after the seismic event without regulations and caution boards; AT4—a tunnel is immediately operable after a seismic event; AT5—the tunnel is operable and remains undamaged by seismic events
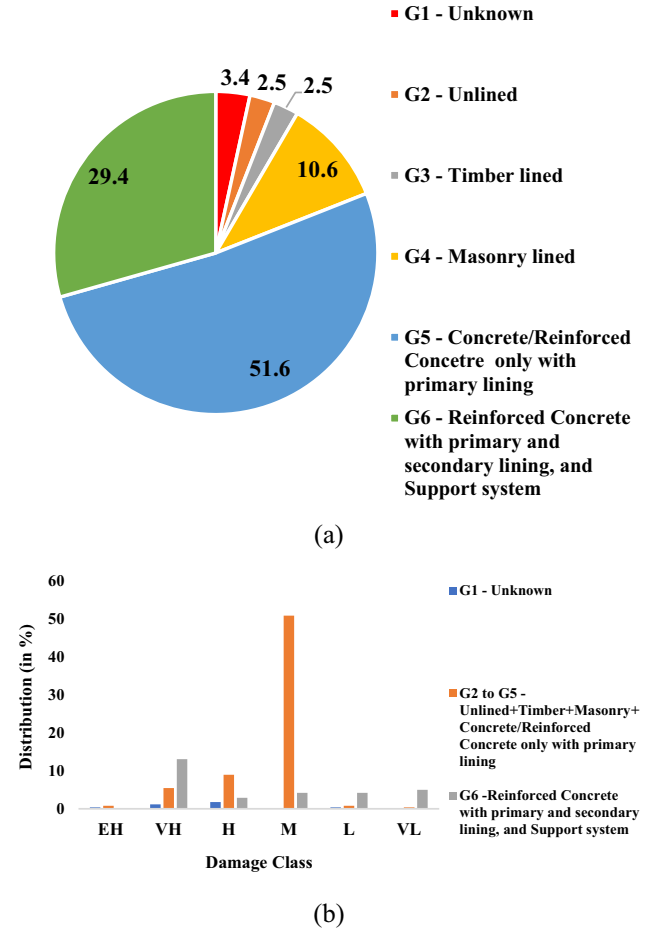
Fig. 6 Distribution of **a** lining types encountered in SDDT (in %) and **b** lining types in each damage class

class for seismic parameters M_w, SSD, PGA, and geological parameters RMR, and OD and probable seismic damages to lining, portal, and invert of the tunnel and accessibility of the tunnel are presented in Table 6. The role of structural parameters (lining type and tunnel's shape) in Table 6 is elaborated in the next sub-section.

3.1.2 Analysis of Influence Parameters: Lining Type and Shape of Tunnel

The order of criticality is obtained for structural parameters like lining type (tunnel linings are the support system of a tunnel which are designed to carry the long-term loads of the tunnel) and the shape of tunnels. A well-defined variation of quantitative values is obtained in each damage class for parameters like PGA, SSD, RMR, and OD, but it is difficult to quantitatively assess the influence of the lining type and shape of tunnels on the seismic response of tunnels. Thus, the order of criticality is obtained for structural parameters for each class based on the research available and SDDT. The term "order of criticality" refers to the severity

of damage in tunnels from higher to lower severity order for lining types and shapes within each damage class. From SDDT, Fig. 6a shows the distribution of number of tunnels (in %) divided into six groups G1 to G6 representing unknown, unlined (UL), timber lined (TL), masonry lined (ML), concrete/reinforced concrete lined only with primary lining as support (CL), and reinforced concrete lined tunnels with primary lining, secondary lining, and support system (RCL), respectively.

The order of criticality for lining types in each damage class is based on the five groups excluding G1 (unknown lining type). Most of the tunnels of the G2, G3, and G4 groups are very old tunnels constructed before the year 1950. A major percentage of the G5 group are tunnels damaged by Kobe, Mid-Niigata, and a few from the Chi-Chi earthquake and others. Most of the G5 group tunnels were constructed on or before the year 1990 as per the database. The G6 group are damaged tunnels from earthquakes like Wenchuan (although few are under construction), Gorkha, Kumamoto, and others. In this study, a peculiar phenomenon related to lining types is observed in each class. The G6 group is considered the best lining group in terms of tunnel performance compared to others. However, the G6 group dominated in the very high (VH) class with 13.1%. Tunnels in the high (H) and moderate (M) damage classes are dominated by G5 followed by G4, G3, and G2. The moderate (M) damage class is dominated by 50% for G2–G5 combinedly and 4.2% for the G6 category. The high (H) damage class is with 9% of G2–G5 combinedly and 3% of the G6 category. The distribution of lining types in each damage class for the G1, G2–G5, and G6 groups is shown in Fig. 6b. Apart from SDDT, a few literature sources are used to propose the order of criticality for lining types in Table 6.

The unlined tunnels (UL) do not provide confinement to the rock mass and are prone to rock fall or rock collapse. Sometimes, the unlined tunnels show slope failure-induced collapse (A21). Two unlined tunnels in the Chi-Chi earthquake (Wang et al. 2001) showed the slope failure-induced collapse. It is concluded that the unlined tunnels are more prone to seismic hazards compared to lined. In older tunnels of this database, timber was used for supporting the tunnel. The Wrights tunnel of this database was timber lined which was damaged in the San Francisco (1906) earthquake reported, the severe damage to the timber lining took place along with complete dislocation as it was passing through a fault zone (Dowding and Rozen 1978). Maidl et al., (2013) discussed the limitation of timber lining that, timber as a material lacks the necessary strength, lacks the bonding with rock mass, produces large deformations under load, and makes it unsuitable for long-term use in tunnel applications. In the early days of tunnel construction, timber was used for initial or temporary support, followed by a permanent brick or stone masonry lining (Maidl et al. 2013). Due to these

reasons, the TL tunnels are marked as the second choice in order of severity. The Pavoncelli tunnel of this database, which is masonry lined, was damaged due to the Irpinia (1980) earthquake. This tunnel suffered from widespread cracks in all the arch and side-wall masonry, with a maximum opening of 4–5 cm cracks, invert uplift, and collapse of part of the roof and side-wall masonry. The main issues with masonry lining stem from its gradual deterioration over time, leading to a loss of strength (Sowden 1990). The structural integrity of a masonry tunnel is highly dependent on the quality of workmanship. Variations in masonry thickness and the presence of voids can compromise the tunnel's strength and durability (Sowden 1990). Even with good supervision, achieving high standards of jointing and bonding throughout the entire length of a tunnel is challenging (Sowden 1990). Thus, the ML tunnels are marked as the third choice in the obtained order of severity.

Timber and brick/masonry materials are largely outclassed by materials like concrete and reinforced concrete which provide superior strength, ductility, durability, and flexibility, making them more suitable for tunnel construction (Sowden 1990). After the mid-twentieth century, tunnel construction shifted from timber and masonry to steel supports and later to rock bolts, shotcrete, and combinations of bolts, steel sets, and shotcrete (a method of applying concrete projected at high velocity) (Steiner 1996). Thus, the next choice in order of severity is CL group tunnels. All of the four lining choices of UL, TL, ML, and CL (G2–G5 group) are seen in the older tunnels group and the G6 group is the one, which is often in practice. The G6 group is RCL tunnels. The G6 group is considered the best in terms of tunnel performance compared to other lining groups. Although G2–G5 group tunnels are old tunnels, they are considered in Table 6. This is because the classification of this study also applies to existing tunnels residing in seismic zones. Numerous recent studies (Llanca et al. 2013, 2017; Atkinson et al. 2021) focus on maintenance and rehabilitation methods to improve the performance of existing masonry tunnels, which were older. Thus, combining the outcomes of a few studies and from the created SDDT, the order of criticality for lining types is decided in Table 6. The order of criticality based on the severity of damage for lining types is UL > TL > ML > CL > RCL, as mentioned in Table 6.

In the SDDT, the observed shapes of the tunnel are Horseshoe (HS), D-shaped (D), ovoid (OV), circular (CR), rectangle (RE), and arched with horizontal roof (AH). In the SDDT, the horseshoe shape is dominated by > 70% of available tunnel data on shapes. Therefore, to overcome the biasness from SDDT, a few other literature sources are used to propose an order of criticality of tunnel shapes in Table 6. From the study of the field investigation of 8 damaged tunnels due to the 1999 Chi-Chi earthquake, Lu and Hwang (2018) have observed that rectangle-like geometry is one

of the major reasons for seismic damage. The rectangle-like geometry of the tunnel caused stress concentrations at the corners, leading to high damage at these locations when subjected to ground shaking. Furthermore, Lu and Hwang (2018) used one of the tunnels (New Sanyi Tunnel) among the damaged tunnels and validated the field investigation by numerical simulations. There are also studies on the seismic behavior of tunnels of different shapes in rocks (Saraswat et al. 2024), the effect of cross-sectional shape on the dynamic response of tunnels under train-induced vibration loads, based on Physical model tests of vibration (Yang et al. 2019) and effect of a blast inside a tunnel for various shapes, based on FE analysis (Goel et al. 2021). These studies proved that cross-sectional shape has a significant effect on the tunnel dynamic behavior.

- Saraswat et al. (2024) have compared the behavior of D-shaped, horseshoe-shaped, and circular tunnels using finite element analysis under both static and seismic conditions, considering different excitation frequencies of harmonic loading. The D-shaped tunnel is the most affected under both static and dynamic conditions, with stress concentration occurring at the corners. The circular shape performs best in both conditions. Consequently, the next best shape is the horseshoe shape (Saraswat et al. 2024).
- The study of Yang et al. (2019) focuses on physical model tests of vibration from three different shaped model tunnels that were performed to study the effects of cross-sectional shape on the dynamic response of tunnels and their surrounding soil. To examine the effects of cross-sectional shape on the tunnel response under the train load, the peak particle acceleration (PPA) of the tunnel at different locations was calculated. The maximum PPA of the rectangular tunnel was 178% of that of the circular tunnel and 133% of the horseshoe-shaped tunnel. The response of the rectangular tunnel was larger than that of both the circular and horseshoe tunnels (Yang et al. 2019).
- In another study by Goel et al. (2021), the FE analysis of shallow underground tunnels (rectangular, circular, and horseshoe tunnels) exposed to a blast inside the tunnel, with surrounding soil media and a structure at ground level, was carried out. The rectangular tunnel had the highest displacement, Von Mises stress, and wave velocity, while the circular tunnel had the lowest. Therefore, it can be concluded that the rectangular shape is more critical for its dynamic responses (Goel et al. 2021).

The major studies described above (Lu and Hwang 2018; Saraswat et al. 2024; Yang et al. 2019; Goel et al. 2021) are based on the dynamic response of rectangular, circular, D, and horse-shoe tunnels. The rectangle shape is considered to be the most critical shape (Lu and Hwang 2018; Yang et al. 2019; Goel et al. 2021) and is marked as a first choice in the order of criticality. The shape like Arched with horizontal roofs (AH) has corners at the top (similar to rectangles at the top portion only), which would again lead to stress concentration at corners. Therefore, it is marked as the second critical shape. Compared to the Horseshoe, the D shape is most affected with stress concentration developing at the corners (Saraswat et al. 2024). Therefore, the D-shape is specifically the preferred third choice as per severity. In the SDDT, a few of the horseshoe-shaped tunnels were damaged as a combination of invert uplift and deformation in the sidewall (A31, A32, and D11 in Table 5). These damaged cases are observed in VH, H, and M damage classes. Therefore, horseshoe-shaped tunnels are marked next severe as per order. The ovoid shape does not have corners or any straight sides and is less likely to be affected by stress concentration. Therefore, the ovoid shape is considered the next choice as per severity. The circular shape is considered best in terms of performance (Saraswat et al. 2024; Yang et al. 2019; Goel et al. 2021). Thus, combining the outcomes of these studies and the created SDDT, the order of criticality for shapes is decided in Table 6. The obtained order is RE > AH > D > HS > OV > CR. The proposed combination in Table 6 will lead to probable seismic damages for each damage class with five parameters, excluding lining type and tunnel shape. However, based on past earthquakes, the proposed order of criticality for linings and shapes from Table 6 can raise engineers' awareness at the planning stage and retrofitting of old tunnel linings for tunnels in seismic zones. When added to seismic and geological parameters, the identified structural parameters, namely lining type and tunnel shape, from this SDDT help create the most comprehensive and complete classification combinations in each damage class.

3.2 Criteria of Seismic Damages Using Critical Combination of Influence Parameters

As the database on seismic damage has already been discussed in Sects. 3.1, 3.1.1, and 3.1.2, we utilized information from the SDDT to create criteria for predicting the seismic damage of tunnels. The criteria are based on the assumption that tunnels with similar parameters to those shown in Table 6, obtained from tunnels in the SDDT, will experience similar damage.

3.2.1 Criteria for Seismic Damages in Each Damage Class from Table 6

EH and VH damage classes The cases in the EH damage class are tunnels near/passing through the ruptured fault

zone. In the VH damage class, a tunnel either passes the fault zone or is very close to the fault zone. The probable damage of EH damage class is A11 and is based on 3 cases. The probable damages of VH damage class are B11, A21, and A31 and they are based on 23, 14, and 11 cases, respectively. In Table 6, the obtained RMR ranges for EH and VH damage classes are 10–25 and 14–40, respectively. The obtained OD ranges for EH and VH damage classes are 30–250 m and 20–300 m, respectively. However, there are a few exception cases of OD in the VH damage class. Three tunnels in the VH damage class are at OD of 400, 550, and 800 m. The order of criticality for the lining type and shape of a tunnel and accessibility of the tunnel in EH and VH damage classes are shown in Table 6. The obtained combination of parameters in the EH damage class of row 1 in Table 6 will lead to A11. The VH damage class in row 2 highlights that, apart from the tunnels passing through the fault zone, the tunnels not passing through the fault zone are also being collapsed and dislocated in lining sections. These tunnels are very close to the fault zone (SSD of 2–5 km). An example of this is S.P.R.R No. 4 and 5 tunnels that were severely damaged/collapsed due to the Kern County earthquake. The obtained combination of parameters in the VH damage class of row 2 in Table 6 will lead to B11, A21, and A31.

H and M damage classes For damage classes H and M, in rows 3 and 4 of Table 6, the fault is not passing through the tunnel. The probable damages of H damage class are B12, C11, and E11 to the lining are based on 6, 10, and 7 cases, respectively, whereas B21 and A32 of portal and invert are based on 10 and 4 cases, respectively. The probable damages of M damage class are C12, D11, and E12 to the lining are based on 47, 25, and 48 cases, respectively, whereas B22 and A33 of portal and invert are based on 18 and 14 cases, respectively. The obtained range of RMR for H and M damage classes is 15–60. The obtained OD ranges for H and M damage classes are 10–200 m and 6–250 m, respectively. Most tunnels in H and M damage classes are at OD < 200 m. Only a few tunnels, in these damage classes are with OD > 200 m. There is an exception of one damage case of 800 m in H class. There are exceptions of two damage cases of OD up to 500 m and one case of 1150 m, respectively in the M damage class. The order of criticality for the lining type and shape of a tunnel and accessibility of the tunnel in H and M damage classes are shown in Table 6. The obtained combination of parameters in the H damage class of row 3 of Table 6 will lead to B12, C11, E11, B21, and A32. The obtained combination of parameters in the M damage class of row 4 of Table 6 will lead to C12, D11, E12, B22, and A33.

L, VL, and EL damage classes For damage classes L and VL, in rows 5 and 6 of Table 6, the tunnel is very far from the ruptured fault zone. The SSDs are higher and PGAs are lower in L and VL damage classes. The probable damages

of L damage class are E13 and B23 to the lining and portal which are based on 7 cases each. The probable damages of VL damage class are E14 and B24 to the lining and portal are based on 11 and 4 cases, respectively. The damage to the invert does not take place for L and VL damage classes. If the PGA is < 0.4 g, the data suggests that the damage to the invert will not take place. The obtained RMR in L and VL damage classes is 40–75 and 40–85, respectively. The obtained OD ranges for L and VL damage classes are 20–400 m and 20–500 m, respectively. A tunnel damaged by the Great Alaskan earthquake (1964) with an OD of 800 m deep in the VL damage class is an exception case. For damage class L in row 5 of Table 6, the combination of obtained parameters will lead to E13 and B23. For damage class VL in row 6 of Table 6, the combination of obtained parameters will lead to E14 and B24. The EL damage class in the 7th row of Table 6 is to show the no-damage scenario. The tunnel remains undamaged at these shaking levels (PGA < 0.01 g) during a seismic event.

3.2.2 A Note on Parameters: RMR and OD

Table 6 provides the summary of the obtained critical combination of parameters and probable damages from SDDT. However, Table 6 cannot have a direct use in the field as it is incomplete. For example: If an engineer is using Table 6 and OD at a site is 300 m, M_w is 7.0, SSD is 30 km, PGA is 0.5 g, RMR is 50, lining type is Cl, and shape is HS, that data of the site corresponds to Moderate (M) damage class except the OD, as the obtained OD for M damage class is 6–250 m. This will lead to confusion in assigning the damage class. Therefore, there are various gaps in Table 6, and is not complete. This sub-section, along with the next one, explains how Table 6 has been further extended and completed to enhance its practical utility in the field. It is observed from Table 6 that except for PGA, all other parameters show overlapping between the damage classes. The objective of this article is to provide unique damage classes for the parameters to be utilized as criteria for obtaining seismic damages in tunnels. To do so, information gathered in Table 6 from SDDT, available literature, and a few assumptions are considered. This sub-section elaborates on parameters RMR and OD on seismic damage of tunnel.

In terms of rock mass conditions, which are represented by RMR in this research, mixed-quality rock mass conditions can be encountered in the tunnels. Both, good and poor-quality rock mass can be observed in one exposed area. However, it is necessary to identify the most critical condition for the assessment of rock mass (Singh and Goel 2011). For example, a fault or a shear zone in a high-quality rock face will play a dominant role, irrespective of the high rock mass strength in the surrounding strata (Bieniawski 1993). Tunnels intersecting fault fracture zones reveal that

Table 7 Criteria for future applicability of critical combination of parameters in each damage class for seismic damage prediction

S. no.	Damage class	Shift in damage class	Parameters							Probable damage			Accessibility of tunnel
			PGA (in g)	M_w*	SSD (in km)	RMR	OD (in m)	Lining type (>)*	Shape (>)**	Lining	Slope/portal	Invert	
1	**Extremely high (EH)**	–	**>1.70**	**6.1–8.0**	**≤2**	**10–25**	**30–250**	**UL>TL>ML>CL>RCL**	**RE>AH>D>HS>OV>CR**	**A11**	**–**	**–**	**AT1**
2	Extremely high (EH)	–*	>1.70	>6.0		1–40	>1	"	"	A11	–	–	AT1
3		Very high (VH)	>1.70	"		41–60	>1	"	"	B11	A21	A31	AT1
4		High (H)	>1.70	"		61–80	>1	"	"	B12 C11 E11	B21	A32	AT2
5		Moderate (M)	>1.70	"		81–100	>1	"	"	C12 D11 E12	B22	A33	AT3
6	**Very high (VH)**	–	**1.70–1.11**	**6.1–8.0**	**≤5**	**14–40**	**20–300**	**UL>TL>ML>CL>RCL**	**RE>AH>D>HS>OV>CR**	**B11**	**A21**	**A31**	**AT1**
7	Very high (VH)	–*	1.70–1.11	>6.0		1–40	>1	"	"	B11	A21	A31	AT1
8		High (H)	1.70–1.11	"		41–60	>1	"	"	B12 C11 E11	B21	A32	AT2
9		Moderate (M)	1.70–1.11	"		61–80	>1	"	"	C12 D11 E12	B22	A33	AT3
10		Low (L)	1.70–1.11	"		81–100	>1	"	"	E13	B23	N	AT4
11	**High (H)**	–	**1.10–0.91**	**6.1–8.0**	**3–15**	**15–60**	**10–200**	**UL>TL>ML>CL>RCL**	**RE>AH>D>HS>OV>CR**	**B12 C11 E11**	**B21**	**A32**	**AT2**
12	High (H)	–*	1.10–0.91	>6.0		1–60	1–800	"	"	B12 C11 E11	B21	A32	AT2
13		Low (L)	1.10–0.91	"		1–60	>800	"	"	E13	B23	N	AT4
14		Moderate (M)	1.10–0.91	"		61–80	1–200	"	"	C12 D11 E12	B22	A33	AT3
15		Low (L)	1.10–0.91	"		61–80	201–800	"	"	E13	B23	N	AT4
16		Very low (VL)	1.10–0.91	"		61–80	>800	"	"	E14	B24	N	AT4
17		Very low (VL)	1.10–0.91	"		81–100	>1	"	"	E14	B24	N	AT4
18	**Moderate (M)**	–	**0.90–0.41**	**6.1–8.0**	**10–65**	**15–60**	**6–250**	**UL>TL>ML>CL>RCL**	**RE>AH>D>HS>OV>CR**	**C12 D11 E12**	**B22**	**A33**	**AT3**
19	Moderate (M)	–*	0.90–0.41	>6.0		1–60	1–500	"	"	C12 D11 E12	B22	A33	AT3
20		Low (L)	0.90–0.41	"		1–60	>500	"	"	E13	B23	N	AT4
21		Low (L)	0.90–0.41	"		61–100	1–250	"	"	E13	B23	N	AT4
22		Very low (VL)	0.90–0.41	"		61–100	>250	"	"	E14	B24	N	AT4
23	**Low (L)**	–	**0.40–0.11**	**6.1–8.0**	**25–110**	**40–75**	**20–400**	**UL>TL>ML>CL>RCL**	**RE>AH>D>HS>OV>CR**	**E13**	**B23**	**N**	**AT4**
24	Low (L)	–*	0.40–0.11	>6.0		1–80	1–400	"	"	E13	B23	N	AT4
25		Very low (VL)	0.40–0.11	"		81–100	1–400	"	"	E14	B24	N	AT4
26		Very low (VL)	0.40–0.11	"		1–100	>400	"	"	E14	B24	N	AT4
27	**Very low (VL)**	–	**0.10–0.01**	**6.1–9.2**	**60–250**	**40–85**	**20–500**	**UL>TL>ML>CL>RCL**	**RE>AH>D>HS>OV>CR**	**E14**	**B24**	**N**	**AT4**

Table 7 (continued)

S. no.	Damage class	Shift in damage class	Parameters							Probable damage			Accessibility of tunnel
			PGA (in g)	M_w*	SSD (in km)	RMR	OD (in m)	Lining type (>)*	Shape (>)**	Lining	Slope/portal	Invert	
28	Very low (VL)	–*	0.10–0.01	>6.0		1–100	1–800	"	"	E14	B24	N	AT4
29	Extremely low (EL)	Extremely low (EL)	0.10–0.01	"		1–100	>800	"	"	N	N	N	AT5
30	**Extremely low (EL)**	–	**<0.01**	**>6.0**	Any	Any	Any	Any	Any	N	N	N	AT5

Remarks: –* in column 3 indicates that the damage class is not shifting and the damage class would be the same as in column 2, M_w*—range of moment magnitude, PGA—peak ground acceleration (in g), SSD—source to site distance (in km), OD—overburden depth (in m), RMR—rock mass rating; (>)*—order of criticality for lining type of the tunnel, UL—unlined, TL—timber lined, ML—masonry lined tunnels (is either only brick or brick and stone work or brick and plain concrete), CL—concrete/reinforced concrete lined tunnels only with primary lining as major support, RCL—reinforced concrete lined tunnels with primary lining, secondary lining, and support system; (>)**—order of criticality for the shape of a tunnel, RE—rectangle, AH—arched with horizontal roof, D—D-shaped, HS—horse Shoe, OV—ovoid, CR—circular. A11—the collapse of a Tunnel; B11 and B12—Grade 1 and Grade 2—lining dislocation, respectively; C11 and C12—Grade 1 and Grade 2—spalling, respectively; D11—lining deformation; E11, E12, E13, and E14—Grade 1, 2, 3, and 4 Lining cracks, respectively; A21—Grade 1—portal/slope damage; b21, B22, B23, and B24—Grade 2, 3, 4, and 5—portal damage, respectively; A31, A32, and A33—Grade 1, 2, and 3—invert damage, respectively; N—no damage. AT1—tunnel cannot be operable after the seismic event; AT2—tunnel is operable after seismic event with many precautions and caution boards; AT3—tunnel is operable after the seismic event without regulations and caution boards; AT4—a tunnel is immediately operable after a seismic event; AT5—the tunnel is operable and remains undamaged by seismic events

the rock mass in these areas is poor and prone to instability (Chen et al. 2023). Many researchers utilized RMR classification for classifying the rock mass of tunnels in the fault zone (Tuğrul 1998; Dalgıç 2003; Kun and Onargan 2013). It showed that after the application of RMR, the rock mass was categorized as very poor (RMR < 20) in many cases and poor in some cases (RMR < 40). In another study (Brideau et al. 2009), the rock mass quality, estimated by the Geological Strength Index (GSI), showed a considerable reduction near tectonic structures. GSI values ranged from < 35 (RMR is < 30) at fault and shear zones, whereas away from these structures, GSI values ranged from 40 to 75 (RMR is 35–70). The study of Martino et al. (2006) found that rock mass quality, quantified by the number of discontinuities per unit volume, increased and the average size of the rock block decreased near faults, and they observed that seismic amplification can occur in fault zones if there is a sharp contrast in rock mass quality between the background rock mass and the fault zone.

Tunnels are long-span structures and during a seismic event, they can sustain multiple damages. Therefore, if a tunnel is undergoing multiple seismic damages, such as lining dislocation, lining spalling, and lining cracks, then the higher amount of damage that occurred in a tunnel is considered as a damage category, and the PSD is noted for every damage category (shown in Table 5). From the proposed SDCT, the amount of damage and PSD decreases for every level of damage class from EH to VL. In EH and VH damage classes, apart from lining dislocation damage due to ruptured fault, the other damages also occurred in the same tunnel. It is evident from Table 6 that the RMR is < 40 at critical fault fracture zones (EH and VH damage classes). Although the fault zone plays a dominant role in tunnel causing collapse or extreme damages as in EH and VH damage classes (from Table 6), seismic damages also occur in tunnels where the rock mass is comparatively better (RMR > 40) as in H, M, L, and VL classes. In the classes where rock mass is in fair to very good rock classes, the amount of damages is lesser, but they are damaged (as per Table 6). Tunnel structures located in poor geological conditions or near faults were particularly vulnerable to seismic damage, especially at fault fracture zones, soft rocks, and the interfaces between soft and hard rocks (Shen et al. 2014; Yu et al. 2016b). At these locations, damage to tunnel structures primarily results from the relative motion of surrounding rock during strong earthquakes. In analyzing six tunnels damaged during the Wenchuan earthquake, Lai et al. (2017) noted that tunnels experienced severe damage in fault fracture zones and soft rock transition sections, while damage in hard rock tunnels was comparatively slight.

To understand and verify the observations of Lai et al. (2017) using the SDDT, data from tunnels in the fault fracture zone, soft rock, and hard rock mass is analyzed. The

percentage of tunnels in the fault fracture zone is 5.3%, Soft Rock is 24.2%, and hard rock is 41.2% for overall rock tunnels. The data was not available for 29.5% of rock tunnels. From the SDDT (as shown in Table 2), the RMR of hard rocks (RMR is 40–60 and RMR was 61–80 when rock class is very good) is typically higher than that of soft rocks (RMR is 15–40). From the proposed SDCT, the amount of damage and PSD decreases for every level of damage class from EH to VL classes. The RMR is also observed to be increasing as the damage class goes from EH to VL classes. This is because EH and VH damage classes were dominated by fault zones and soft rocks, respectively whereas the H and M damage classes are dominated by soft and hard rock-based tunnels (RMR of 15–60), and L and VL damage classes were dominated by hard rock-based tunnels (RMR of 40–75 and 40–85). The study finds similar observations with Lai et al. (2017) in terms of rock mass and fault fracture zone and verifies with this study. This SDDT indicates that with increasing RMR, seismic damage to the tunnel decreases.

In the SDDT, maximum OD of tunnel is 1150 m which is a Melamchi tunnel residing in the Moderate (M) damage class. The study by Shrestha et al. (2020) emphasized that seismic damages to the Melamchi tunnel were spalling (13%) and lining cracks (87%). Shrestha et al. (2020) mentioned that the highest proportion of severe damage patterns in the Melamchi tunnel occurred at an OD of 0–300 m. Based on six damaged tunnels of the Wenchuan earthquake, Lai et al. (2017) observed that tunnels, with OD of 25 m, experienced serious seismic damage. As tunnel OD increased, the seismic damage decreased and tunnels with OD > 500 m showed little seismic damage (Lai et al. 2017). In the Tawarayama tunnel with an OD of 300 m, the maximum number of damages occurred at depths less than 150 m (Zhang et al. 2020). A study by Sharma and Judd (1991) suggested a critical OD limit of < 50 m for causing seismic damage. Yu et al. (2016b) found that the tunnels suffered lesser seismic damage when OD is > 40 m compared to OD of 1–40 m. From Table 6 of this study, the maximum OD limit observed is 500 m in VL damage class. All the damage classes of SDDT are dominated by tunnels with maximum OD's < 300 m followed by a range of 300–500 m cases, except a few are at > 500 m. This study finds similar observations to other studies related to the influence of OD in seismic damage of tunnels (Sharma and Judd 1991; Yu et al. 2016b; Lai et al. 2017; Zhang et al. 2020; Shrestha et al. 2020). This SDDT indicated that with increasing tunnel depth, seismic damage to tunnels generally decreased. The deeper tunnels (OD > 500 m) appear safer from seismic damage compared to shallow tunnels (OD < 500 m) as per SDDT. However, the Longxi tunnel (maximum OD of 800 m and in VH damage class of this study) damaged during the

Wenchuan earthquake is an exception, where a deep tunnel suffered very high damage.

3.2.3 Criteria for Future Applicability of Combination of Parameters from Table 7

The various gaps in Table 6 are filled by introducing Table 7 in this study. PGA values are dependent on M_w and SSD. Table 6 was based on PGA ranges for M_w of 6.1 to 9.2 for the VL damage class and 6.1 to 8 for remaining damage classes. For using Table 7, this study recommends the use of region-based attenuation relationships for obtaining PGA at the site. Table 7 modifies M_w to > 6.0 for all damage classes. Obtaining the distance from the source to the tunnel site, and the potential M_w of the source can be used in the region-based attenuation relationships, to calculate the PGA. This overcomes the limitation for values of $M_w > 8.0$ also, which was not accounted for in Table 6. Therefore, this study recommends that for $M_w > 6.0$, irrespective of the SSD range, the obtained PGA value should be used for selecting the damage class from Table 7. Three things utilized in forming Table 7 for parameters RMR and OD are the above observations from this study and comparison with other studies/literature (mentioned in Sect. 3.2.2), Table 6 of this study, and a few assumptions. The order of criticality for lining type and shape of the tunnel remains the same in Table 7 for the damage classes as it remained in Table 6. The accessibility of tunnel for each row is shown in the last column of Table 7. Table 7 overcomes the limitation of Table 6 and the damage class can be successfully assigned to a tunnel site by Table 7. Table 7 provides completeness to Table 6 and enhances the future utility at tunnel sites for understanding SVRT before an earthquake. In Table 7, the rows with rows: 1, 6, 11, 18, 23, and 27 which are bolded are the parameters, probable damages, and accessibility of tunnel for each damage class which are from Table 6. Below these rows, the exceptions are added for $M_w > 6.0$, order of criticality of lining type, shape of tunnel, accessibility of tunnel, and PGA ranges (in g) for > 1.70, 1.70–1.11, 1.10–0.91, 0.90–0.41, 0.40–0.11, 0.10–0.01, and < 0.01. The 30th row in Table 7 is to show the negligible damage scenario of the tunnel, where M_w is modified to > 6.0. In Table 7, the maximum RMR limits to 100. Each damage class and their shifts in damage classes of Table 7 are elaborated below.

EH and VH damage classes and their shifts in damage classes In Table 6, for the EH damage class the PGA is > 1.70 g. The obtained RMR range is 10–25 and OD of 30–250 m. The seismic damages of the EH and VH damage classes are due to the close vicinity of a tunnel near the faults. Numerous researchers (Tuğrul 1998; Dalgıç 2003; Brideau et al. 2009; Kun and Onargan 2013) have reported that near the faults the values of RMR are in the range of

1–40. Hence, 2nd row and 7th row of Table 7 consider a range of RMR from 1–40. OD is modified based on the Longxi tunnel having an OD of 800 m in the VH damage class, which suggests that even at higher OD, tunnels are vulnerable to seismic damage in the EH and VH class. Thus, OD is considered > 1 m for EH and VH damage class as given in Table 7 of rows two to five and rows seven to ten. Therefore, the 2nd row of Table 7 corresponds to predicting A11 for RMR of 1–40, OD of > 1 m with PGA > 1.70 g.

The higher RMR value (RMR > 40) reduces seismic damage to tunnels as explained by Wang et al. (2001) and Lai et al. (2017), causing a downward shift in damage classes from EH to EL as given in Table 6. However, the data available in SDDT is insufficient to provide the range of RMR for the other downward-shifted damage classes observed for the PGA > 1.7 g. The study assumes the RMR ranges according to RMR classes given by Bieniawski (1993) to mark the downward shift in the damage classes as given in Table 7 (3rd–5th row). The proposed boundaries are subject to change in the future if the proposed boundaries are unable to predict the seismic damage to a tunnel. It is proposed that the RMR of 41–60, the PGA is > 1.70 g, and OD is > 1 m given in the 3rd row of Table 7, the damage class shifts downward from EH to VH predicting probable damages as B11, A21, and A31 to lining, portal, and invert, respectively. In the same manner, when RMR is 61–80, the rock class is better than poor, very poor, and fair rock classes as proposed by Bieniawski (1993) and the damage class further shifts to H. Therefore, in the 4th row of Table 7, when RMR is 61–80 and PGA is > 1.70 g, OD is > 1 m for H damage class predicting probable damages as B12, C11, E11, to lining and B21, and A32 for portal, and invert, respectively. Likewise in the fifth row of Table 7, RMR is increased to 81–100, and the damage class further shifts to M predicting probable damages as C12, D11, E12, to lining, B22, and A33 for portal and invert, respectively.

In Table 6, for the VH damage class, the PGA is 1.70–1.11 g. The obtained RMR range is 14–40 and OD of 20–300 m. The predicted damages are B11, A21, and A31. Table 6 is a summary of the created SDDT. The 7th row of Table 7 is an extension based on the observation already mentioned above for the EH damage class. In the 7th row, the parameters range are RMR 1–40, OD > 1 m, and PGA 1.70–1.11 g for VH damage class corresponding to B11, A21, and A31 types of damages. If rock class increases from poor to fair, the RMR values increase to 41–60 as given by Bieniawski (1993) and the amount of seismic damage to the tunnel decreases with a higher RMR. As RMR is increased to 41–60, the amount of damage decreases causing the downward shift of the damage class, where the VH class shifts to the H damage class. Therefore, for RMR of 41–60, PGA of 1.70–1.11 g, and the OD is > 1 m given in the 8th row of Table 7, the damage class shifts to H damage class

predicting probable damages as B12, C11, E11 to the lining, whereas B21 and A32 of portal and invert, respectively. Likewise, if the RMR is increased to 61–80, the amount of damage further decreases, and the damage class shifts to M damage class predicting C12, D11, E12 to the lining, whereas B22 and A33 of portal and invert, respectively as provided in row 9 of Table 7. In the same manner, if the RMR is increased to 81–100, the amount of damage further decreases and the damage class shifts to L damage class predicting E13 and B23 to the lining and portal, respectively as shown in row ten of Table 7. Thus, when the $M_w > 6.0$, PGA > 1.70 g and 1.70–1.11 g, OD > 1 m, RMR of 1–100, with the order of criticality of lining type, shape, and accessibility of tunnel is complete. The 2nd—5th rows and 7th—10th rows in Table 7 overcome the limitation of row 1 and row 6 of Table 7 which are basically row 1 and row 2 of EH and VH classes in Table 6.

H and M damage classes and their shifts in damage classes From Table 6, the damage cases of damage classes H and M are the one's with fault not passing through the tunnel. Most tunnels in H and M damage classes are at OD < 200 m. There are exceptions of damage cases up to 800 m in H damage class and 500 m in M damage classes as mentioned in Sect. 3.2.1. Table 7 extends the OD cases of H damage class by considering OD up to > 800 m and shows the impact of damage with varying RMR values for PGA of 1.10–0.91 g. Likewise, Table 7 extends the OD cases of M damage class by considering OD up to > 500 m and shows the impact of damage with varying RMR values for PGA of 0.90–0.41 g. From the proposed SDCT, amount of damage and PSD decrease for each damage class from EH to VL. By comparing with other studies (Sharma and Judd 1991; Yu et al. 2016b; Lai et al. 2017; Zhang et al. 2020; Shrestha et al. 2020) and observations of this study suggest that with increasing tunnel depth, seismic damage generally decreases and higher RMR correlates with reduced seismic damage. These observations and a few assumptions are utilized to provide completeness to H and M damage classes and their shifts in damage classes through Table 7.

In Table 6, for the H damage class, the PGA is 1.10–0.91 g. The obtained RMR range is 15–60 and OD of 10–200 m. Table 6 is a summary of the created SDDT and predicted damages of H damage class are B12, C11, E11 to the lining, whereas B21 and A32 of portal and invert, respectively. For PGA of 1.10–0.91 g, this study considers that, if the RMR is in range of 1–14 and OD is 1–9 m, practically the damage would remain the same as B12, C11, E11 to the lining, whereas B21 and A32 of portal and invert, respectively. The OD range is considered up to 800 m in 12th row of Table 7, based on the exception case in SDDT. Therefore, 12th row of Table 7 corresponds to predicting B12, C11, E11, B21, and A32 for ranges of RMR of 1–60, OD of 1–800 m with PGA 1.10–0.91 g. In the same manner,

keeping all the parameters same as row twelve of Table 7 and if the OD is increased to > 800 m, the amount of damage further decreases, and damage class shifts to L damage class predicting E13 and B23 to the lining and portal, respectively as given in row thirteen of Table 7. In 13th row of Table 7, the probable damages are minimal as the OD is higher, which is > 800 m. Similarly, if RMR is 61–80, the rock class is good, which is better than poor, very poor, and fair rock classes as proposed by Bieniawski (1993). If RMR is increased, the amount of seismic damage decreases. Therefore, for PGA of 1.10–0.91 g, if RMR is 61–80, OD is 1–200 m, damage class shifts to M damage class predicting C12, D11, E12 to the lining, whereas B22 and A33 of portal and invert, respectively as shown in 14th row of Table 7. In the same manner, keeping all the parameters same as row fourteen of Table 7 and if the OD is increased to 201–800 m, the amount of damage further decreases, and damage class shifts to L damage class predicting E13 and B23 to the lining and portal, respectively as provided in row fifteen of Table 7. Likewise, keeping all the parameters same as 15th row of Table 7 and if the OD is further increased to > 800 m, the amount of damage further decreases, and damage class shifts to VL damage class predicting E14 and B24 to the lining and portal, respectively as given in 16th row of Table 7. VL class predicts the minimal forms of seismic damage to a tunnel. Hence, for PGA of 1.10–0.91 g, if RMR is 81–100, the OD limit is not differentiated and considered as > 1 m which would predict E14 and B24 to the lining and portal, respectively as given in row seventeen of Table 7.

In Table 6, for the M damage class, the PGA is 0.90–0.41 g. The obtained RMR range is 15–60 and OD of 6–250 m. Table 6 is a summary of the created SDDT and predicted damages of M damage class are C12, D11, E12 to the lining, whereas B22 and A33 of portal and invert, respectively. For PGA of 0.90–0.41 g, this study considers that even if the RMR is at a range of 1–14 and if OD is at 1–5 m also, practically the damage would remain the same as C12, D11, E12 to the lining, whereas B22 and A33 of portal and invert, respectively. The OD range is considered up to 500 m in the 19th row of Table 7, based on the exception of two cases in SDDT. Therefore, 19th row of Table 7 corresponds to predicting C12, D11, E12, B22, and A33 for RMR of 1–60, OD of 1–500 m with PGA 0.90–0.41 g. Similarly, keeping all the parameters same as row 19 of Table 7 and if the OD is increased to > 500 m, the amount of damage further decreases, and damage class shifts to L damage class predicting E13 and B23 to the lining and portal, respectively as shown in row twenty of Table 7. The study by Shrestha et al. (2020) supports the previous statement as the Melamchi Tunnel with OD of 1150 m, included in the SDDT, experienced lining cracks, classified as E13 as per this SDCT, at an OD > 500 m, as indicated in row twenty of Table 7. Correspondingly, if the RMR is increased to 61–100, the

rock class is good to very good, which is better than poor, very poor, and fair rock classes as proposed by Bieniawski (1993). If RMR is increased, the amount of seismic damage decreases. Therefore, for PGA of 0.90–0.41 g, RMR of 61–100, OD is 1–250 m, the amount of damage decreases and damage class shifts to L damage class predicting E13 and B23 to the lining and portal, respectively as provided in 21st row of Table 7. Correspondingly, keeping all the parameters same as row 21 of Table 7 and if the OD is increased to > 250 m, the amount of damage further decreases, and damage class shifts to VL damage class predicting E14 and B24 to the lining and portal, respectively as given in 22nd row of Table 7. The RMR of 61–100 is considered in 21st and 22nd rows instead of 61–80 and 81–100 because L and VL damage classes predict minimal forms of seismic damage to a tunnel. Therefore, without differentiating the good and very good rock classes, they are combined here as the damages are minimal. E14 and B24 are the least damage types that could occur to a tunnel. Thus, for $M_w > 6.0$, PGA of 1.10–0.91 g and 0.90–0.41 g, OD combinations for > 1 m, RMR of 1–100, with an order of criticality of lining type, shape, and accessibility of tunnel are complete. The 12th–17th rows and 19th–22nd rows in Table 7 overcome the limitation of row 11 and row 18 of Table 7 which are basically row 3 and row 4 of H and M damage classes of Table 6.

L, VL, and EL damage classes and their shifts in damage classes The damage classes L and VL have lesser PGA compared to other damage classes. In Table 6, for the L damage class, the PGA is 0.40–0.11 g, the obtained RMR range is 40–75, and the OD of 20–400 m. The predicted damages are E13 and B23 to the lining and portal, respectively. Table 6 is a summary of the created SDDT. For PGA of 0.40–0.11 g, this study assumes that even if the RMR is in the range of 1–39, 76–80, and if OD is at 1–19 m also, practically the damage would remain the same as E13 and B23. Therefore, the 24th row of Table 7 corresponds to predicting E13 and B23 for RMR of 1–80, OD of 1–400 m with PGA of 0.40–0.11 g. In the same manner, keeping all the parameters same as row 24 of Table 7 and if the RMR is increased to 81–100, the amount of damage further decreases, and damage class shifts to VL damage class predicting E14 and B24 to the lining and portal, respectively as given in the 25th row of Table 7. Likewise, if RMR is 1–100 and OD is increased to > 400 m for PGA of 0.40–0.11 g, the damage class shifts to VL damage class predicting E14 and B24 to the lining and portal, respectively as provided in 26th row of Table 7. Here, the RMR of 1–100 is considered instead of 1–80 and 81–100 because, if the damage class is shifting, then the VL damage class is predicted, which is the least form of seismic damage to a tunnel. Therefore, without differentiating the rock classes, they are combined here.

In Table 6, for the VL damage class, the PGA is 0.10–0.01 g. The obtained RMR range is 40–85 and OD of

20–500 m. Table 6 shows a summary of the created SDDT and predicted damages are E14 and B24 to the lining and portal, respectively. For PGA of 0.10–0.01 g, even if the RMR is at a range of 1–39, 85–100, and if OD is at 1–19 m also, practically the damage would remain same as E14 and B24. The OD range is considered up to 800 m in 28th row of Table 7, based on one exception case in SDDT. Therefore, 28th row of Table 7 corresponds to predicting E14 and B24 for RMR of 1–100, OD of 1–800 m with PGA of 0.10–0.01 g. Correspondingly, keeping all the parameters same as the 28th row of Table 7 and OD is increased to > 800 m, the amount of damage further decreases, and damage class shifts to EL damage class predicting N, which represents no damage caused as given in 29th row of Table 7. Thus, for $M_w > 6.0$, PGA of 0.40–0.11 g and 0.10–0.01 g, OD combinations for > 1 m, RMR of 1–100, with order of criticality of lining type, shape, and accessibility of tunnel are complete. The 24th–26th rows and 28th and 29th rows in Table 7 overcomes the limitation of row 23 and row 27 of Table 7 which are basically row 5 and row 6 of L and VL damage classes of Table 6.

The EL damage class has PGA values of < 0.01 g, $M_w > 6.0$, and irrespective of any other parameter, it predicts the no damage scenario as provided in row thirty of Table 7, which is basically the 7th row of the EL damage class of Table 6. Therefore, the critical combination of parameters for predicting probable seismic damage from Table 7 provides the completeness of parameters with various combinations. Thus, based on observations of this study and literature, a few assumptions and outcomes of Table 6, Table 7 is formed. The shifts in Table 7 are important because using the current study in the field provides an early advantage in determining the need for seismic-related investigations for a tunnel. However, Table 7 is subjected to change or refinement when more data gets added.

3.2.4 Role of Other Parameters in the Seismic Performance of the Tunnel

Apart from the seven parameters of Table 6 in this study, the literature reports that other four parameters like the length of the tunnel, lining thickness, method of construction, and age of tunnels also account for the seismic damage of the tunnel (Dowding and Rozen 1978; Jiang et al. 2010; Chen et al. 2012; Yu et al. 2017). Longer lengths of tunnels undergo the intersection of different rocks or rock masses and different strata (Yu et al. 2017). In Sect. 4, the methodology for predicting seismic damage before the earthquake is elaborated. It is mentioned that, for tunnels, the SSD from the sources is obtained from any end of the portal for tunnel lengths < 2 km and further the PGA values can be sorted

from higher to lower order for all sources within 250 km. For the tunnels with lengths > 2 km, it is recommended to obtain the SSD from the most critical section of rock mass (least RMR value or interface of rock mass or weak/shear zones in the tunnel). If there are multiple critical sections in long tunnels, the multiple SSDs are considered and the PGA values can be sorted from higher to lower order for all sources within 250 km. However, in the long tunnels, when they undergo the intersection of different rocks or rock mass, the combinations of RMR are also accounted for in Table 7 along with seismic and structural parameters. Therefore, the effect of the length of the tunnel is indirectly accounted for through the parameter RMR and the proposed methodology in this study. From the study of Chen et al. (2012), the New Austrian Tunneling Method (NATM) is considered as better than other methods of construction based on tunnel conditions after the earthquake. However, it was observed from SDDT that the G6 group/RCL lining type which is the preferred lining in NATM shows lower cases of damage as compared to others. Indirectly the order of criticality of lining type in the classification is taking care of this aspect.

The study of Jiang et al. (2010) mentioned that a higher degree of seismic damage in tunnels is associated with the higher age of the lining. The age is obtained by subtracting the year of seismic damage from the year of commencement of a tunnel. The deterioration of tunnel linings is typically seen due to aging (Asakura and Kojima 2003). The maintenance, inspection, diagnosis, and repair technologies of tunnels are essential for ensuring the safety of these aging infrastructures (Asakura and Kojima 2003). The maintenance, inspection, diagnosis, and repair of tunnels are associated with many uncertainties, which the present study in its current form ignores. The study of Dowding and Rozen (1978) concluded that seismic damage in tunnels is higher for larger lining thicknesses (≥ 40 cm). The general tunnel practice ignores seismic loads on the lining (Wang et al. 2001; Li 2012; Chen et al. 2012; Shen et al. 2014; Yu et al. 2016b; Zhang et al. 2018; Shrestha et al. 2020). Hence, this implies that the tunnel linings are designed for static loads (ITA 1988). In general, the lining thickness is the function of RMR, OD, and in-situ stress ratio. Lower RMR results in higher lining thickness in design and this study shows tunnels in lower RMR are more prone to seismic damage. Therefore, the two parameters, RMR and OD, indirectly account for the effects of lining thickness in the present study. Therefore, the length of the tunnel, lining thickness, method of construction, and age of tunnels are not accounted for explicitly in Table 6 of this study. The methodology for predicting damage before the earthquake and validation are elaborated in Sect. 4.

Fig. 7 Methodology for predicting the seismic damage in tunnels before earthquake
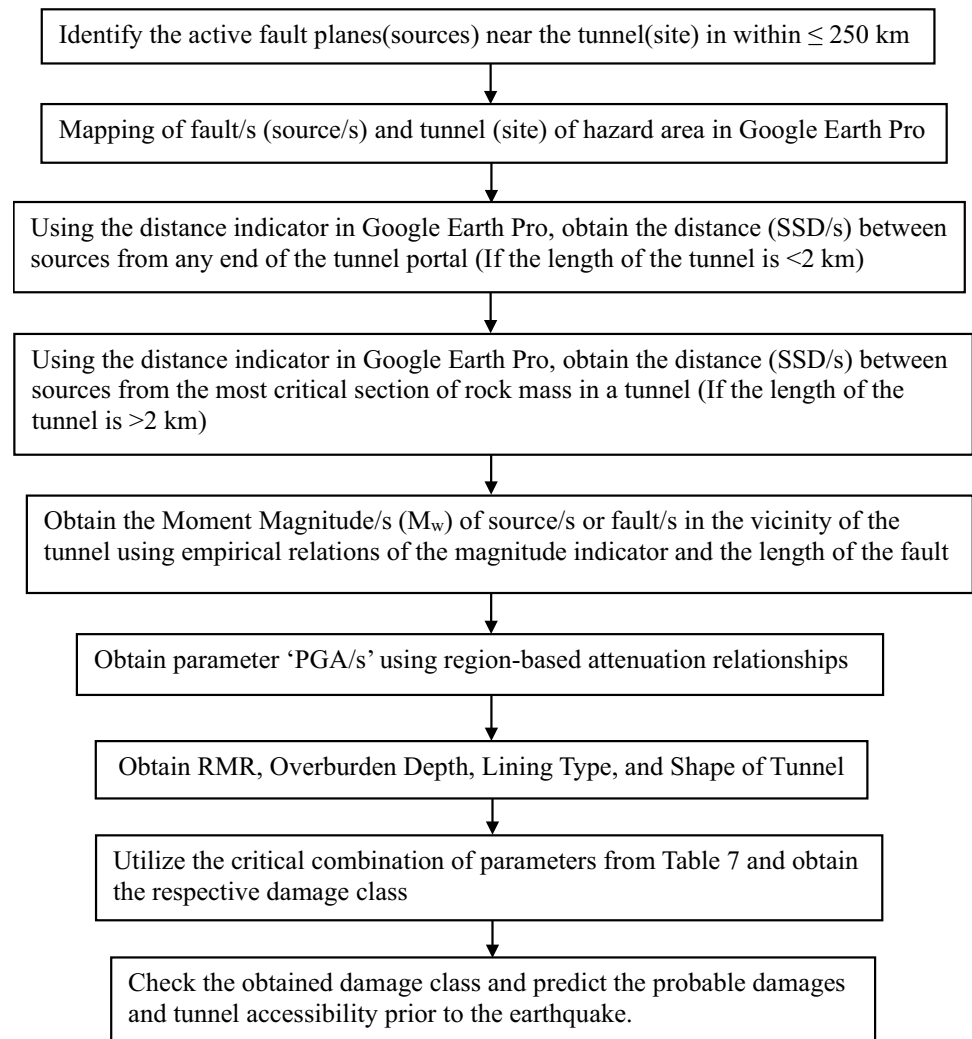
4 Methodology for Predicting Seismic Damage in Tunnels Before Earthquake

The previous section describes on utilization of Tables 6 and 7, which provide a summary of SDDT and insights into predicting potential seismic damage of tunnels, respectively. From this, a simplistic methodology is proposed for damage assessment and prediction before earthquakes for existing and future tunnels as shown in Fig. 7.

If a tunnel(site) is residing in a seismic zone, the initial step is to identify the active faults (sources) near the tunnel. From Table 6, for the VL damage class, the upper limit of SSD is 250 km. Thus, the sources within 250 km are of interest, from the site. The distance between the sources and the site of interest is to be obtained. The distance from the sources is obtained from any end of the portal for tunnel lengths < 2 km. For the tunnels with lengths > 2 km, it is recommended to obtain the SSD from the most critical section of rock mass (least RMR value or interface of rock mass or weak/shear zones in the tunnel). If there are

multiple critical sections in tunnels with lengths > 2 km, multiple SSDs are to be obtained. Map the location of a site and sources in Google Earth Pro. Using the distance indicator tool in Google Earth Pro, the SSD is calculated. If the tunnel is passing through the active fault plane (sources), the SSD is very low. Along with SSD, the M_w of a source is to be obtained. Empirical relationships on magnitude indicators proposed by Wells and Coopersmith (1994) as tabulated in Table 8 are used to obtain the magnitude of sources. These empirical relationships are correlated between M_w and surface rupture length. Studies of worldwide earthquakes show that faults do not rupture over their entire lengths or areas during individual events. Instead, individual fault segments with physically controlled boundaries rupture repeatedly (Kramer 1996).

After obtaining SSD and M_w, the PGA of the tunnel site is calculated using the region-based attenuation relationships. This study is based on 26 different earthquakes causing damage to the tunnels. Thus, the adopted region-based attenuation relationships of this study can be used

Table 8 Empirical relationships between moment magnitude (M_w), and surface rupture length (L in km) (after Wells and Coopersmith 1994)

Fault movement	Number of events	Relationship	Standard deviation (σ_{Mw})
Strike-slip	43	$M_w = 5.16 + 1.12 \log L$	0.28
Reverse	19	$M_w = 5.00 + 1.22 \log L$	0.28
Normal	15	$M_w = 4.86 + 1.32 \log L$	0.34
All	77	$M_w = 5.08 + 1.16 \log L$	0.28

in future hazard analyses of tunnels at respective seismic hazard areas. The attenuation relationships of PGA (PHA) for rock sites are to be considered. After obtaining PGA, other critical parameters of Table 7 are to be obtained. For example, if three active faults are present in the vicinity of the tunnel, three SSDs, Magnitudes, and PGAs are obtained as (SSD1, SSD2, SSD3), (M1, M2, M3) and (PGA1, PGA2, PGA3). From all three sources, the PGA's and SSDs might differ and predicted damage class and probable damages also differ from those three faults when they are critically combined with other parameters. This helps in identifying and knowing, which damage is caused by the respective fault/s in the tunnel vicinity. From this methodology and SDCT, the damage to the rock tunnel is predicted before an earthquake using Table 7 and Fig. 7. Hence, this simplistic methodology can be utilized by engineers at a site to know the seismic vulnerability of the rock tunnel before an earthquake. It neither requires any rigorous calculations nor AI or ML techniques.

## 4.1 Validation of Proposed SDCT and Methodology

On February 6th, 2023, two major earthquakes took place in the East Anatolian Fault Zone (~700 km long) of Türkiye. Due to this earthquake, there was damage to the Erkenek Tunnel in Türkiye. This tunnel site is utilized for validation of the proposed SDCT and Methodology. The Mainshock of M_w-7.8 (Pazarcık) took place on EAFZ and was initiated at Narli Fault. Nine hours later another event of M_w-7.5 (Elbistan) took place on the Surgu-Cardak faults. The rupture surface of these events was roughly 300 and 160 km long representing left-lateral strike-slip motion for both events. The focal depth of these events is 10 and 7.4 km. The mapping is done in Google Earth Pro for the ruptured fault models, epicenters of both earthquakes and Erkenek tunnel, as shown in Fig. 8a, b. The red lines represent the surface trace of the fault models of both earthquakes. The epicenters of M_w-7.8 and 7.5 are represented in red and yellow-colored star shapes, respectively and Erkenek tunnel is red-colored T notation. A Portal Start and Portal End of Tube 1 and 2 (PST1, PET1, and PST2, PET2)

are mapped (white-colored line), as shown in Fig. 8b. The details of the Erkenek tunnel are mentioned in Table 9. The details of rock units present at the site, rock mass, geometry, and lining types are obtained from the literature mentioned in Table 9. The SSD is obtained from both the ends of portal, as shown in Fig. 8b. The OD is unknown from any report. However, it was obtained as 25–160 m by mapping the elevation profile along the tunnel path in Google Earth Pro. For obtaining PGA, the GMPE of Akkar et al. (2014) is used. Although this GMPE applies to Europe and the Middle East, its database is dominated by recordings of Türkiye, Italy, and Greece and is applicable for M_w 4.0–8.0 and focal depths ≤ 30 km.

Based on Table 9, the parameters of the tunnel are as follows: M_w of 7.8, SSD range of 3.5 and 4.1 km with PGA values of 0.969 and 0.939 for portal ends. The site parameters like RMR are between 24 and 29, and the maximum OD of the tunnel is 160 m. The tunnel is horseshoe-shaped, and reinforced concrete is the lining type. If all these parameters (M_w, SSD, PGA, RMR, OD, tunnel's shape, and lining type) are combined, they correspond to row 3 of Table 6/ row 11 of Table 7 with damage class High (H). As per this combination of parameters, the probable damages are B12, C11, E11, B21, and A32. From the reports (GEER and EERI Report 2023; Aydan and Ulusay 2023), the actual damages in twin tubes are compiled as shown in Fig. 9a–f.

It is observed that the actual damages are very close to the predicted ones as per this study. The damages in Fig. 9a–d are lining damages referring to B12, C11, and E11, whereas Fig. 9e, f are close to B21, and A32 as per this SDCT and description of Table 5. In Erkenek Tunnel's case, one of the tubes was closed after inspection on 6th February 2023 and another one was in operation. By March 20th, 2023, both the tunnel tubes were open to traffic as per GEER and EERI report (2023). As per row 3 of Table 6, the tunnel is operable after seismic event with many precautions and necessary caution boards. In terms of accessibility as well, this study predicted the outcome correctly. Another reason for highlighting the proposed methodology is that it would have predicted similar damage, even if it were before an earthquake. The magnitude indicator (as per Table 8) of EAFZ ~700 km long is M_w of 8.3 (± 0.28). For the indicated M_w and SSD (~3.5 to 4.0), the maximum PGA (calculated as per Akkar et al. 2014) would be 0.99 g. For this PGA and other parameters as a combination, it would still fall under the same damage class of high (H) and would predict similar damages. Thus, the efficacy of the proposed methodology is detailed and checked for the Erkenek tunnel.

Fig. 8 Google Earth Pro image of **a** mapping of the ruptured fault, epicenters of the Kahramanmaraş earthquake sequence, and damaged Erkenek tunnel (Source of KMZ file for fault rupture: USGS), **b** Mapping of Erkenek twin tunnel tubes and their portals
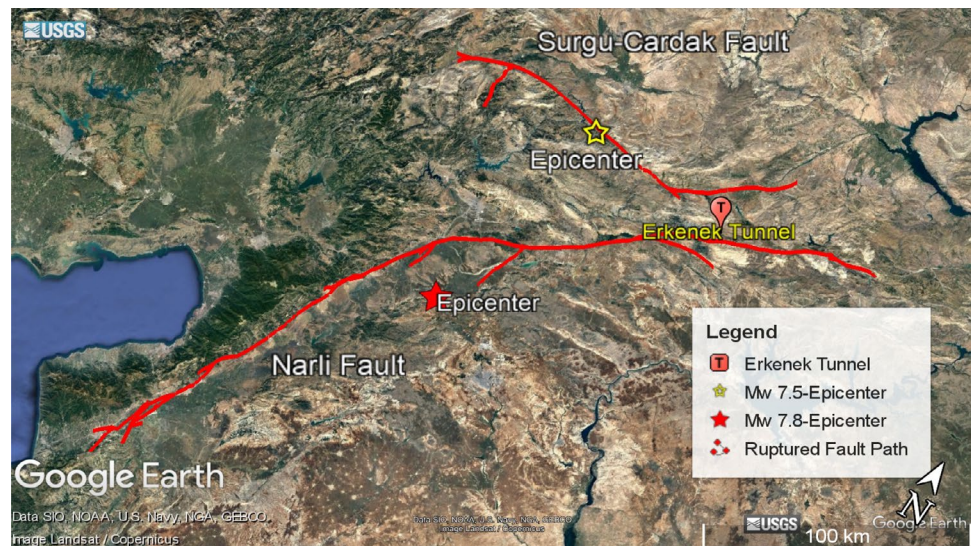
(a)
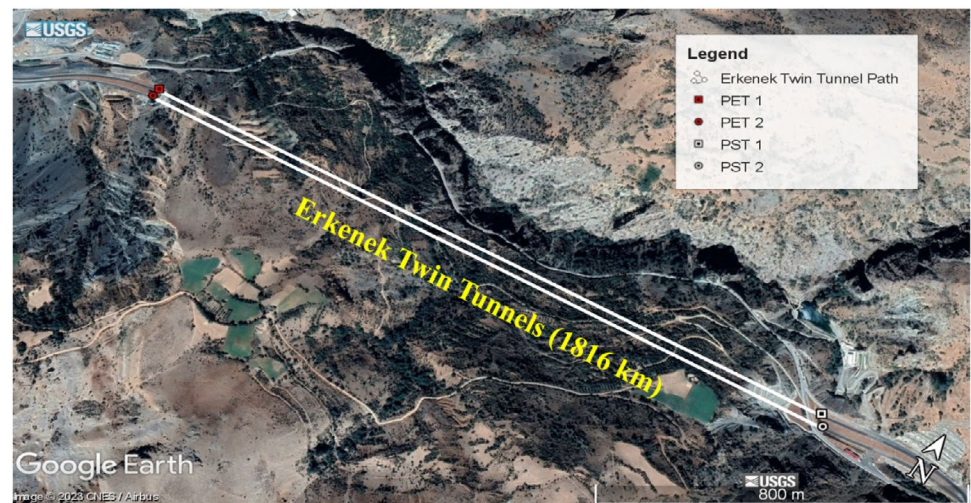
(b)

5 Discussion

The proposed SDCT based on lining, portal, and invert utilizes PGA as a prominent seismic parameter and does not use PGV as a majority of region-based attenuation relations are available only for PGA. This is the first study that uses region attenuation relations for obtaining PGA for tunnels. The attenuation relationships are based on peak horizontal acceleration values and vertical seismic motion is considered to have a minor effect on the seismic response of tunnels based on a study by Yu et al. (2016a). The effect of vertical seismic motion on the seismic response of tunnels can be better understood through more detailed numerical analysis in future studies. Numerous seismic damage classifications of tunnels are available, but they are modified for every event based

on the amount of damage and all of them are based on forensic analysis. For the first time, the SDCT and proposed methodology can be used before the earthquake also without using any rigorous calculations or any AI or ML techniques. The prominence of this study lies in the simplicity of utilizing this methodology at sites by rock and tunnel engineers all over the world before an earthquake. The proposed SDCT could not accommodate damage like groundwater leakage. The leakage is due to leaks in the concrete lining and is associated with either lining cracks or spalling, which is detailed in Table 5. The proposed SDCT assumes seismic-resistant design is not considered in tunnels. This study is limited to categorizing the damage and the role of influence parameters with their critical combination responsible for the damage. This study does not propose any retrofitting techniques, improvements to

Table 9 Details of the Erkenek tunnel in Türkiye

Name of tunnel	Erkenek tunnel
Location (latitude, longitude)	(PST1/PST2-37.9232, 37.8888) and (PET1/PET2-37.9231, 37.8660)
Geometry of tunnel	10.30×7.47 m (width × height), 1816 m (Length) (Gokceoglu and Karahan 2023)
Tunnel type	Road tunnel (twin tube)
SSD1, SSD2 (in km)	3.5 (from PST 1 and PST 2)*, 4.1 (from PET 1 and PET 2)*
Region attenuation used	Akkar et al. (2014)
Calculated PGA (in g)	0.969 (for SSD1), 0.939 (for SSD2)
Rock units	Graphitic schist, calcschists, recrystallized limestones (Gedik 2021)
RMR	24–29 (poor) (Gedik 2021)
Maximum OD (in m)	160
Lining type	Reinforced concrete (C25/C30—C stands for concrete, and the numeric value is the strength of the concrete) (lining thickness—40 cm) (support system details are unknown) (Gokceoglu and Karahan 2023)
Shape	Horse-Shoe

Remarks: *—(PST1, PET1, and PST2, PET2)—a portal start and portal end of tubes 1 and 2

(a)   (b)   (c)   (d)   (e)   (f)

Fig. 9 **a**, **b** Spalling of concrete linings, **c** a portion of the roof and sidewall damage, **d** longitudinal cracking, **e** traces of rockfall above the portals, **f** pavement dislocation at the entrance of the portal (Source: GEER and EERI Report 2023; Aydan and Ulusay 2023)

the lining types, seismic isolation methods or so. Utilizing this SDCT, for every damage class, separate retrofitting measures and mitigation measures can be developed in the future.

The proposed combination in Table 7 can predict probable seismic damages for each damage class by using the other five parameters excluding lining type and tunnel shape. However, considering past earthquakes, the suggested order of criticality of linings and shapes in Table 7 can raise awareness among engineers' during the planning stages and retrofitting of old tunnel linings for tunnels in seismic zones. For different cases of each damage class in Table 7, the lining types and shapes can be analyzed by numerical analysis which provides a better understanding and can lead to improvements in Table 7. A numerical analysis of a three-dimensional geological model that incorporates seismic and rock mass parameters of tunnel sites will provide deeper insights. This study accounts for obtaining quantitative values for seismic parameters like M_w, SSD, and PGA. However, to understand the influence of seismic waveform changes and the presence of impulse waves in seismic damage to the tunnel, a numerical analysis is recommended. There are no cases of tunnel damage for $M_w < 6.1$ as per SDDT. This study is based on created SDDT from the records of actual damaged tunnel sites. Therefore, Table 7 adjusts the utility of M_w on-site by marking $M_w > 6.0$, regardless of SSD. The region-based attenuation relationship should be utilized to obtain the PGA value for selecting the damage class from Table 7. The proposed boundaries for parameters in Table 7 are subject to change in the future if the proposed boundaries cannot predict the seismic damage to a tunnel. This study is based on data of damaged tunnel sites and it is subject to change or refinement when more data gets added. One should prefer a site-specific numerical analysis for a detailed overview of the seismic response of tunnels considering the actual geological and structural conditions of the site. However, using the current methodology provides

a head start in deciding the requirement for such seismic-related investigation for a tunnel.

6 Conclusions

This study is unique in its way, by differentiating the roles of seismic, structural, and geological parameters in each damage class. An extensive literature review is conducted to create the global largest SDDT from 235 tunnel sites damaged by 26 earthquakes. This formed a basis for establishing SDCT and methodology for predicting damage before an earthquake. The validation of the proposed methodology showed a good agreement with the Erkenek Tunnel in Türkiye. This SDCT is the first of its kind which can be utilized for pre-seismic damage assessment of tunnels. This study can provide insight for tunnel engineers all over the world, about the importance of parameters like M_w, PGA, SSD, RMR, OD, lining types, and shape of the tunnel at the planning stage or before the construction of a tunnel in a seismic zone. It also provides a rapid post-seismic damage description after an earthquake as it covers the minimal form of damage like cracking or stones piling up in front of a portal to major damages like collapse and lining dislocations. The proposed methodology is very simple to use as it does not involve any complex numerical analysis or rigorous calculations or any other AI/ML techniques. This study provides a clear overall outlook on the role of each parameter in the damage response of tunnels and can be used as a guideline for seismic damage assessment of tunnels. Hence, the proposed methodology can be implemented for existing, old, new, and upcoming tunnels residing in a seismic zone for seismic damage assessment. This article has a follow-up as part 2, where by using this method, a Python-based GUI tool is developed for India and adjacent countries. Initially, the data of seismic sources from India and adjacent countries are collected. The collected seismic sources serve as input data. Then, a Python code is written to identify the sources within 250 km of the tunnel site and also calculates the PGA from each source through empirical attenuation relationships. The input parameters to be entered in this GUI-tool are latitude and longitude (user's location), RMR, OD in m, tunnel lining type, and tunnel shape. Critically combining all these parameters, the software predicts the damage class and probable damages from seismic sources within 250 km of the study region of a user. The reports are generated in.txt (notepad) format and include graphs showing the distribution of total faults in each damage class. Engineers can obtain the SVRT in India and nearby countries through this software before an earthquake.

Declarations

References

Akkar S, Sandıkkaya MA, Bommer JJ (2014) Empirical ground-motion models for point-and extended-source crustal earthquake scenarios in Europe and the Middle East. Bull Earthq Eng 12:359–387. https://doi.org/10.1007/s10518-013-9461-4

Ansari A, Rao KS, Jain AK, Ansari A (2023) Deep learning model for predicting tunnel damages and track serviceability under seismic environment. Model Earth Syst Environ 9(1):1349–1368. https://doi.org/10.1007/s40808-022-01556-7

Argyroudis SA, Pitilakis KD (2012) Seismic fragility curves of shallow tunnels in alluvial deposits. Soil Dyn Earthq Eng 35:1–12. https://doi.org/10.1016/j.soildyn.2011.11.004

Asakura T (1996) Mountain tunnels performance in the 1995 Hyogoken-Nanbu earthquake. Special report of the 1995 Hyogoken-Nanbu earthquake

Asakura T, Kojima Y (2003) Tunnel maintenance in Japan. Tunn Undergr Space Technol 18(2–3):161–169. https://doi.org/10.1016/S0886-7798(03)00024-5

Asakura T, Sato Y (1996) Damage to mountain tunnels in hazard area. Soils Found 36:301–310. https://doi.org/10.3208/sandf.36.Special_301

Atkinson C, Paraskevopoulou C, Miller R (2021) Investigating the rehabilitation methods of Victorian masonry tunnels in the UK. Tunn Undergr Space Technol 108:103696. https://doi.org/10.1016/j.tust.2020.103696

Aydan O, Ulusay R (2023) A quick report on Pazarcik and Ekinözü Earthquakes (Türkiye) of February 6, 2023

Aydan Ö, Ohta Y, Geniş M, Tokashiki N, Ohkubo K (2010) Response and stability of underground structures in rock mass during earthquakes. Rock Mech Rock Eng 43:857–875. https://doi.org/10.1007/s00603-010-0105-6

Bieniawski ZT (1993) Classification of rock masses for engineering: the RMR system and future trends. In: Rock testing and site characterization, pp 553–573. https://doi.org/10.1016/B978-0-08-042066-0.50028-8

Bradley BA (2013) A New Zealand-specific pseudospectral acceleration ground-motion prediction equation for active shallow crustal earthquakes based on foreign models. Bull Seismol Soc Am 103(3):1801–1822. https://doi.org/10.1785/0120120021

Brideau MA, Yan M, Stead D (2009) The role of tectonic damage and brittle rock fracture in the development of large rock slope failures. Geomorphology 103(1):30–49. https://doi.org/10.1016/j.geomorph.2008.04.010

Campbell KW, Bozorgnia Y (2008) NGA ground motion model for the geometric mean horizontal component of PGA, PGV, PGD and 5% damped linear elastic response spectra for periods ranging

from 0.01 to 10 s. Earthq Spectra 24(1):139–171. https://doi.org/10.1193/1.2857546

Chen Z, Wei J (2013) Correlation between ground motion parameters and lining damage indices for mountain tunnels. Nat Hazards 65:1683–1702. https://doi.org/10.1007/s11069-012-0437-5

Chen Z, Shi C, Li T, Yuan Y (2012) Damage characteristics and influence factors of mountain tunnels under strong earthquakes. Nat Hazards 61:387–401. https://doi.org/10.1007/s11069-011-9924-3

Chen Z, Yan Q, Zhou Z, He C, Li T, Bao Y (2023) Stability analysis and deformation control of tunnel with extremely weak surrounding rocks caused by strike-slip fault activity. Rock Mech Rock Eng 56(12):8543–8569. https://doi.org/10.1007/s00603-023-03513-x

Corigliano M, Lai CG, Barla G (2007) Seismic vulnerability of rock tunnels using fragility curves. In: 11th ISRM congress. OnePetro

Cui Z, Sheng Q, Zhang GM, Liu H (2021) A modified rock mass classification considering seismic effects in the basic quality (BQ) system. Bull Eng Geol Environ 80:2249–2260. https://doi.org/10.1007/s10064-020-02064-7

Dalgıç S (2003) Tunneling in fault zones, Tuzla tunnel, Türkiye. Tunn Undergr Space Technol 18(5):453–465. https://doi.org/10.1016/S0886-7798(03)00045-2

Dowding CH, Rozen A (1978) Damage to rock tunnels from earthquake shaking. J Geotech Eng Div 104(2):175–191. https://doi.org/10.1061/AJGEB6.0000580

Gedik A (2021) Measures taken on road tunnel portals in landslide sections: case of Erkenek tunnel, Malatya. In: Proceeding of international congress of engineering and natural sciences studies (ICENSS2021), May 07–09 2021 Ankara/Türkiye, pp 248–281 (in Turkish)

GEER (Geotechnical Extreme Events Reconnaissance Association) and EERI (Earthquake Engineering Research Institute), and Association Report 082, LFE Program (2023) Türkiye earthquakes: report on geoscience and engineering impacts. https://doi.org/10.18118/G6PM34

Goel MD, Verma S, Mandal J, Panchal S (2021) Effect of blast inside tunnel on surrounding soil mass, tunnel lining, and superstructure for varying shapes of tunnels. Undergr Space 6(6):619–635. https://doi.org/10.1016/j.undsp.2021.01.003

Gokceoglu C, Karahan S (2023) Seismic performance of transportation tunnels in the region affected by the 6 February 2023 Türkiye earthquake sequence: a general assessment. In: 57th U.S. rock mechanics/geomechanics symposium, ARMA 23-0960. https://doi.org/10.13140/RG.2.2.19031.85928

Hashash YM, Kim B, Olson SM, Ahmad I (2012) Seismic hazard analysis using discrete faults in Northwestern Pakistan: Part I–methodology and evaluation. J Earthq Eng 16(7):963–994. https://doi.org/10.1080/13632469.2012.681423

Hoek E, Brown ET (1997) Practical estimates of rock mass strength. Int J Rock Mech Min Sci 34(8):1165–1186. https://doi.org/10.1016/S1365-1609(97)80069-X

Huang J, Zhao X, Zhao M, Du X, Wang Y, Zhang C, Zhang C (2020) Effect of peak ground parameters on the nonlinear seismic response of long-lined tunnels. Tunn Undergr Space Technol 95:103175. https://doi.org/10.1016/j.tust.2019.103175

ITA, Working Group on General Approaches to the Design of Tunnels (1988) Guidelines for the design of tunnels. Tunn Undergr Space Technol 3(3):237–249. https://doi.org/10.1016/0886-7798(88)90050-8

Jiang Y, Wang C, Zhao X (2010) Damage assessment of tunnels caused by the 2004 Mid Niigata Prefecture earthquake using Hayashi's quantification theory type II. Nat Hazards 53:425–441. https://doi.org/10.1007/s11069-009-9441-9

Kanno T, Narita A, Morikawa N, Fujiwara H, Fukushima Y (2006) A new attenuation relation for strong ground motion in Japan based on recorded data. Bull Seismol Soc Am 96(3):879–897. https://doi.org/10.1785/0120050138

Kramer SL (1996) Geotechnical earthquake engineering. Pearson Education India

Kun M, Onargan T (2013) Influence of the fault zone in shallow tunneling: a case study of Izmir metro tunnel. Tunn Undergr Space Technol 33:34–45. https://doi.org/10.1016/j.tust.2012.06.016

Lai J, He S, Qiu J, Chen J, Wang L, Wang K, Wang J (2017) Characteristics of seismic disasters and aseismic measures of tunnels in Wenchuan earthquake. Environ Earth Sci 76:1–19. https://doi.org/10.1007/s12665-017-6405-3

Li T (2012) Damage to mountain tunnels related to the Wenchuan earthquake and some suggestions for aseismic tunnel construction. Bull Eng Geol Env 71:297–308. https://doi.org/10.1007/s10064-011-0367-6

Lin PS, Lee CT (2008) Ground-motion attenuation relationships for subduction-zone earthquakes in northeastern Taiwan. Bull Seismol Soc Am 98(1):220–240. https://doi.org/10.1785/0120060002

Lin PS, Lee CT, Cheng CT, Sung CH (2011) Response spectral attenuation relations for shallow crustal earthquakes in Taiwan. Eng Geol 121(3–4):150–164. https://doi.org/10.1016/j.enggeo.2011.04.019

Llanca D, Breul P, Bacconnet C, Sahli M (2013) Characterization of the masonry lining of an underground structure by geoendoscopy. Tunn Undergr Space Technol 38:254–265. https://doi.org/10.1016/j.tust.2013.07.009

Llanca D, Breul P, Bacconnet C (2017) Improving the diagnosis methodology for masonry tunnels. Tunn Undergr Space Technol 70:55–64. https://doi.org/10.1016/j.tust.2017.07.002

Lu CC, Hwang JH (2018) Damage analysis of the new Sanyi railway tunnel in the 1999 Chi-Chi earthquake: necessity of second lining reinforcement. Tunn Undergr Space Technol 73:48–59. https://doi.org/10.1016/j.tust.2017.12.009

Lu H, Li Y, Chen M, Kim H, Serikawa S (2018) Brain intelligence: go beyond artificial intelligence. Mob Netw Appl 23:368–375. https://doi.org/10.1007/s11036-017-0932-8

Maidl B, Thewes M, Maidl U (2013) Handbook of tunnel engineering I, 1st edn. Wiley. Available at: https://www.perlego.com/book/1001994/handbook-of-tunnel-engineering-i-structures-and-methods-pdf. Accessed: 28 June 2024

Martino S, Minutolo A, Paciello A, Rovelli A, Mugnozza GS, Verrubbi V (2006) Evidence of amplification effects in fault zone related to rock mass jointing. Nat Hazards 39:419–449. https://doi.org/10.1007/s11069-006-0001-2

Montaldo V, Faccioli E, Zonno G, Akinci A, Malagnini L (2005) Treatment of ground-motion predictive relationships for the reference seismic hazard map of Italy. J Seismol 9:295–316. https://doi.org/10.1007/s10950-005-5966-x

Nguyen DD, Park D, Shamsher S, Nguyen VQ, Lee TH (2019) Seismic vulnerability assessment of rectangular cut-and-cover subway tunnels. Tunn Undergr Space Technol 86:247–261. https://doi.org/10.1016/j.tust.2019.01.021

Owen GN, Scholl RE (1981) Earthquake engineering of large underground structures, prepared for the Federal Highway Administration. FHWAIRD-801195

Özbey C, Sari A, Manuel L, Erdik M, Fahjan Y (2004) An empirical attenuation relationship for northwestern Türkiye ground motion using a random effects approach. Soil Dyn Earthq Eng 24(2):115–125. https://doi.org/10.1016/j.soildyn.2003.10.005

Qiu W, Huang G, Zhou H, Xu W (2018) Seismic vulnerability analysis of rock mountain tunnel. Int J Geomech 18(3):04018002. https://doi.org/10.1061/(ASCE)GM.1943-5622.0001080

Rahmati A, Faramarzi L, Sanei M (2014) Development of a new method for RMR and Q classification method to optimize support

system in tunneling. Front Struct Civ Eng 8:448–455. https://doi.org/10.1007/s11709-014-0262-x

Ramkrishnan R, Sreevalsa K, Sitharam TG (2021) Development of new ground motion prediction equation for the North and Central Himalayas using recorded strong motion data. J Earthq Eng 25(10):1903–1926. https://doi.org/10.1080/13632469.2019.1605318

Roy N, Sarkar R (2017) A review of seismic damage of mountain tunnels and probable failure mechanisms. Geotech Geol Eng 35:1–28. https://doi.org/10.1007/s10706-016-0091-x

Rozen A (1977) Response of rock tunnels to earthquake shaking. Doctoral dissertation, Massachusetts Institute of Technology

Sadigh K, Chang CY, Egan JA, Makdisi F, Youngs RR (1997) Attenuation relationships for shallow crustal earthquakes based on California strong motion data. Seismol Res Lett 68(1):180–189. https://doi.org/10.1785/gssrl.68.1.180

Saraswat S, Maheswari BK (2024) Seismic behaviour of tunnels of different shapes in rocks. Jpn Geotech Soc Spec Publ 10(20):730–735. https://doi.org/10.3208/jgssp.v10.OS-9-0

Sarmiento A, Madugo D, Bozorgnia Y, Shen A, Mazzoni S, Lavrentiadis G, Dawson T, Madugo C, Kottke A, Thompson S, Baize S (2021) Fault displacement hazard initiative database. In: Fault displacement hazard initiative database, Report GIRS-2021-08. https://doi.org/10.34948/N36P48

Sharma S, Judd WR (1991) Underground opening damage from earthquakes. Eng Geol 30(3–4):263–276. https://doi.org/10.1016/0013-7952(91)90063-Q

Shen Y, Gao B, Yang X, Tao S (2014) Seismic damage mechanism and dynamic deformation characteristic analysis of mountain tunnel after Wenchuan earthquake. Eng Geol 180:85–98. https://doi.org/10.1016/j.enggeo.2014.07.017

Shinji M, Akagi W, Shiroma H, Yamada A, Nakagawa K (2002) JH method of rock mass classification for tunnelling. In: ISRM international symposium-EUROCK 2002. OnePetro

Shrestha R, Li X, Yi L, Mandal AK (2020) Seismic damage and possible influencing factors of the damages in the Melamchi tunnel in Nepal due to Gorkha earthquake 2015. Geotech Geol Eng 38:5295–5308. https://doi.org/10.1007/s10706-020-01364-9

Singh B, Goel RK (2011) Engineering rock mass classification (1755–1315). Butterworth-Heinemann, Boston

Sowden AM (ed) (1990) The maintenance of brick and stone masonry structures, 1st edn. CRC Press, Boca Raton. https://doi.org/10.1201/9781003062066

Steiner W (1996) Tunnelling in squeezing rocks: case histories. Rock Mech Rock Eng 29(4):211–246. https://doi.org/10.1007/BF01042534

Tuğrul A (1998) The application of rock mass classification systems to underground excavation in weak limestone, Atatürk dam. Türkiye Eng Geol 50(3–4):337–345. https://doi.org/10.1016/S0013-7952(98)00034-9

Wang ZZ, Zhang Z (2013) Seismic damage classification and risk assessment of mountain tunnels with a validation for the 2008 Wenchuan earthquake. Soil Dyn Earthq Eng 45:45–55. https://doi.org/10.1016/j.soildyn.2012.11.002

Wang WL, Wang TT, Su JJ, Lin CH, Seng CR, Huang TH (2001) Assessment of damage in mountain tunnels due to the Taiwan Chi-Chi earthquake. Tunn Undergr Space Technol 16(3):133–150. https://doi.org/10.1016/S0886-7798(01)00047-5

Wang Z, Gao B, Jiang Y, Yuan S (2009) Investigation and assessment on mountain tunnels and geotechnical damage after the Wenchuan earthquake. Sci China Ser E Technol Sci 52:546–558. https://doi.org/10.1007/s11431-009-0054-z

Wells DL, Coppersmith KJ (1994) New empirical relationships among magnitude, rupture length, rupture width, rupture area, and surface displacement. Bull Seismol Soc Am 84(4):974–1002. https://doi.org/10.1785/BSSA0840040974

Wu A, Zhao W, Zhang Y, Fu X (2023) A detailed study of the CHN-BQ rock mass classification method and its correlations with RMR and Q system and Hoek–Brown criterion. Int J Rock Mech Min Sci 162:105290. https://doi.org/10.1016/j.ijrmms.2022.105290

Xu H, Xu J, Sun R, Pu H, Cheng Y (2021) Rapid assessment and classification for seismic damage of mountain tunnel based on concentric circle method. Shock Vib 2021:1–16. https://doi.org/10.1155/2021/9944797

Yang W, Zhang C, Liu D, Tu J, Yan Q, Fang Y, He C (2019) The effect of cross-sectional shape on the dynamic response of tunnels under train induced vibration loads. Tunn Undergr Space Technol 90:231–238. https://doi.org/10.1016/j.tust.2019.05.006

Yashiro K, Kojima Y, Shimizu M (2007) Historical earthquake damage to tunnels in Japan and case studies of railway tunnels in the 2004 Niigataken-Chuetsu earthquake. Quart Rep RTRI 48(3):136–141. https://doi.org/10.2219/rtriqr.48.136

Youngs RR, Chiou SJ, Silva WJ, Humphrey JR (1997) Strong ground motion attenuation relationships for subduction zone earthquakes. Seismol Res Lett 68(1):58–73. https://doi.org/10.1785/gssrl.68.1.58

Yu H, Chen J, Bobet A, Yuan Y (2016a) Damage observation and assessment of the Longxi tunnel during the Wenchuan earthquake. Tunn Undergr Space Technol 54:102–116. https://doi.org/10.1016/j.tust.2016.02.008

Yu H, Chen J, Yuan Y, Zhao X (2016b) Seismic damage of mountain tunnels during the 5.12 Wenchuan earthquake. J Mt Sci 13:1958–1972. https://doi.org/10.1007/s11629-016-3878-6

Yu H, Yuan Y, Bobet A (2017) Seismic analysis of long tunnels: a review of simplified and unified methods. Undergr Space 2(2):73–87. https://doi.org/10.1016/j.undsp.2017.05.003

Zhang X, Jiang Y, Sugimoto S (2018) Seismic damage assessment of mountain tunnel: a case study on the Tawarayama tunnel due to the 2016 Kumamoto Earthquake. Tunn Undergr Space Technol 71:138–148. https://doi.org/10.1016/j.tust.2017.07.019

Zhang X, Jiang Y, Maegawa K (2020) Mountain tunnel under earthquake force: a review of possible causes of damages and restoration methods. J Rock Mech Geotech Eng 12(2):414–426. https://doi.org/10.1016/j.jrmge.2019.11.002

Zhang B, Yu Y, Li X, Wang Y (2022) Ground motion prediction equation for the average horizontal component of PGA, PGV, and 5% damped acceleration response spectra at periods ranging from 0.033 to 8.0 s in southwest China. Soil Dyn Earthq Eng 159:107297. https://doi.org/10.1016/j.soildyn.2022.107297